DEMOCRATIC AND POPULAR REPUBLIC OF ALGERIA
MINISTRY OF HIGHER EDUCATION AND SCIENTIFIC RESEARCH
MOHAMED BOUDIAF UNIVERSITY – M'SILA

FACULTY OF TECHNOLOGY
DEPARTMENT OF ELECTRICAL ENGINEERING
ORDER NO : ELM-13

DOMAIN : SCIENCE AND TECHNOLOGY
SPECIALITY : ELECTROMECHANICAL
OPTION : ELECTROMECHANICAL

THE BRIEF THAT WAS SUBMITTED TO OBTAIN FROM THE ACADEMIC MASTER'S DEGREE

By : - Mohamed Ali MADI
- Lotfi HIMEUR

THESIS

STUDY OF AN ELECTRICAL ENERGY PRODUCTION SYSTEM COUPLING A PHOTOVOLTAIC FIELD

Dissertation Committee:

Dr. Hilal RAHALI	Mohamed Boudiaf University – M'sila	President
Dr. Toufik ROUBACHE	Mohamed Boudiaf University – M'sila	Supervisor
Dr. Riyadh ROUABHI	Mohamed Boudiaf University – M'sila	Examiner

Academic year : 2023/2024

Thanks

We thank Allah the giving us the courage, the will, and the patience to complete this present work.

We would like to thank our supervisor Mr.Roubache Toufik for proposing a very interesting topic and for his advice, for his availability and for sharing his knowledge and qualities, both professionally and personally.

Our respect and gratitude also go to the members of the jury who honored us by evaluating this work and whose availability, observations, and reports allowed us to enrich our work.

We are grateful to all the teachers who have helped us learn from a young age until now.

We thank all the people who have participated directly or indirectly in the realization of this work.

Dedication

No words can fully express the gratitude, love, respect, and appreciation I feel. Simply put: I dedicate this modest work:

To my dear mother ***Noura****: You represent for me the source of tenderness and the epitome of dedication, constantly encouraging me. You have done more than any mother could to ensure that her children follow the right path in life and in their studies.*

To my dearest father ***Mourad****: no dedication can fully express the love, esteem, devotion, and respect I have always had for you. Nothing in the world compares to the efforts you have made day and night for my education and well-being. This work is the fruit of the sacrifices you have made for my education and development over the years.*

To my dearest brothers and sister: ***Soheyb, Youcef*** *and* ***Sarah***

To my dearest friends,

To all my colleagues and companions with whom I have shared my educational journey,

To all my teachers since my early years of study,

To all those dear to me whom I have forgotten to mention.

Lotfi HIMEUR

Dedication

No words can fully express the gratitude, love, respect, and appreciation I feel. Simply put: I dedicate this modest work:

To my dear mother ***Fatima****: You represent for me the source of tenderness and the epitome of dedication, constantly encouraging me. You have done more than any mother could to ensure that her children follow the right path in life and in their studies.*

To my dear and late father ***Ahmed (Allah Yarhmo)****: There is no dedication that can fully express the love, appreciation, sincerity and respect I have always enjoyed for you. Nothing in the world compares to the efforts that I have made day and night for my education and well-being. This work is the fruit of the sacrifices I have made for my education and development over the years.*

To all my family

To my dearest friends, clans

To all my colleagues and companions with whom I have shared my educational journey,

To all my teachers since my early years of study,

To all those dear to me whom I have forgotten to mention.

MADI MOHAMED ALI

Contents

List of Figures

List of Tables

List of symbols

L: Inductance of a single winding (bobinage).

Ms - Mr: Mutual inductance coupling between stator windings/ rotor windings.

C: electromagnetic torque of machine. [N.m]

Cs: The resisting torque (static) on the machine shaft [N.m].

$\boldsymbol{J}$: Inertia moment [Kg.m^2]

f: Coefficient of friction [N.m/rad/s].

P: The number of pole pairs

« o »: Homopolar axis index

Ls - Lr: Stator cyclic inductance / rotor cyclic inductance.

M: Cyclic mutual inductance between stator and rotor.

Cr: Resistance torque.

σ: Total leakage coefficient.

θ: position of the rotor relative to the stator.

S(x): Sliding Surface.

λ : the wavelength [m].

Isc: short-circuit current.

G: irradiance.

m: mass of the moving parts.

K: damping constant.

Vt: thermal voltage (V).

Ns: Number of PV cells connected in series.

Io: saturation current. It depends on the junction temperature (A).

Rs: series resistance, which represents various resistances of metallic contacts and connections. It is very low (Ω).

Rsh: shunt resistance (much higher compared to Rs). A low Rsh, will have an impact on the open-circuit voltage. It characterizes the leakage current at the junction (Ω).

$Iscn$: nominal short-circuit current (A)

Ki: temperature coefficient of short-circuit current (A/K) or (A/°C)

T: operating temperature (K)

Tn: nominal temperature (298 K)

Gn: irradiance under standard conditions (Gn =1000W/m2)

Vo: the open-circuit voltage

V: the thermal voltage

Kv: the coefficient of temperature for open-circuit voltage (V/K) or (V/°C)

$V \quad cn$: the nominal open-circuit voltage (V)

a: the ideality factor of the junction, ranging between 1 and 2.

q: the charge of an electron ($q = 1.6 \times 10{-}19C$)

C_{em}: represents the electromagnetic motor torque.

C_l: represents the load torque.

ω: represents the angular velocity.

X: distance from the point to the centre of rotation,

M: The rotating mass,

R: The maximum radius of the steering wheel,

K: A coefficient of form that takes different values according to the geometry of the steering wheel

ρ: The volumetric mass density, which is 7850 kg/m³ for the above-mentioned ELMS, is used to calculate the inertia of the components.

L: the height of the cylinder considered.

Ω: rotation speed

λ: Positive coefficient.

x_d: Desired value.

T_{32}^{T}: Three-phase to two-phase transformation matrix (Concordia).

X: State vector.

U: Input vector.

θ, ω Angular position and velocity of the dq frame relative to the αβ frame in an AC machine.

ψ: Magnetic flux.

a, b, c Components along the three-phase axes a, b, and c

α,β Components along the two-phase axes α and β

d,q Components along the two-phase axes d and q

ω: Electrical rotational speed

List of abbreviations

ASM: Asynchronous Motor.

SMC: Sliding Mode Control.

VSC: Variable Structure Command.

MPP: Maximum power point.

MPPT: Maximum Power Point Tracking.

DC: Direct current.

PV: Photovoltaic.

PVG: Photovoltaic generator.

AC: alternating current.

HF: High frequence.

PWM: Pulse Width Modulation

MOSFET: Metal Oxide Semiconductor Field Effect Transistor

P&O: Perturbation and Observation (Perturb & Observ)

General introduction

Since the widespread of the use of electricity, global energy consumption is growing very fast worldwide. Consumption will continue to increase either in electrical or economic terms [1], [2].

Renewable energies (wind, sun, biomass, water disturbance) are all natural and unlimited resources that can be used to generate electricity [3].

Today, the sun is an inexhaustible and clean energy source. It could cover several thousand times of energy compared to other global energy resources.

The geographical location of Algeria favors a large deposit of the sun (the long duration of sunshine, the high intensity of radiation). The region of Adrar is considered among the wilayas that have a great solar potential throughout the year, where the sunshine exceeds eight (8) hours in the summer season. Also, the property of the deserted Algerian company encourages the large-scale use of solar energy, either on a public scale (seven (7) photovoltaic plants are installed and put into service with a power generated of 53 Mwatt, public lighting, etc.), or on a personal scale represented by the extensive use of photovoltaic pumping. This reflects an ambition to forecast the exploitation of geographical conditions to increase the use of solar energy in the region.

The global scheme of our work is an electromechanical system coupling to a photovoltaic field. The storage system is composed of an asynchronous motor and a cylindrical steel flywheel coupled to a synchronous generator.

Asynchronous machines are commonly used in industrial settings for driving pumps, fans, compressors, and conveyor systems due to their reliability and low maintenance requirements. It does not require a separate excitation power source, making them simpler in design compared to synchronous machines.

A flywheel is a mechanical device used to store rotational energy. It consists of a heavy rotating wheel with a significant moment of inertia. When coupled with an asynchronous machine, a flywheel can store excess energy generated during periods of low demand or from renewable energy sources like wind or solar. The rotational inertia of the flywheel allows it to maintain a relatively constant speed, providing a stable rotational energy source.

The generator synchronous is typically coupled with the flywheel to convert its rotational energy into electrical energy. It can be synchronous or asynchronous depending on the specific requirements of the system. The electrical energy generated by the generator can be utilized to power electrical loads directly or stored in batteries for later use.

Overall, coupling an asynchronous machine with a flywheel and generator offers a versatile solution for energy storage and stabilization in various industrial and power systems applications.

This thesis is divided into three chapters as follows:

The first chapter represents generalities on the various renewable energy systems and especially photovoltaic solar energy by giving an overview on the PV effect and the cell that is the heart of the solar panel to define the field and the generator photovoltaic. A study of an electromechanical system, for the production of electrical energy, which represents various examples, such as: asynchronous machine, and flywheel.

The second chapter concerns the modeling of a PV and the various machines used in this system, it is all about equations and some descriptions of these machines.

Then, in the third chapter, we will present the control and the energy-autonomous photovoltaic bench with energy storage.

Finally, we will end this thesis with general conclusions and some perspectives for future work.

Chapter I

The different renewable production resources and the electromechanical system

I.1. Introduction

Nowadays, the use of renewable energy sources to generate power has become widely spread across the world. Renewable energy refers to a group of energy sources that are endless on a human scale, widely available, essentially free, and compliant with specific environmental standards. They may be transformed into power as needed [4]. Renewable energy (sometimes called green energy) is recycled or regenerated on the scale of a human life.

It may be called clean energy because it is produced by PV modules, which does not result in waste or contaminate the environment. However, this resource has two drawbacks: production is always dependent on weather conditions, and a vast surface area is required to create huge amounts of energy due to the poor efficiency of PV panels.

This chapter also has another part that consists of the electromechanical system because the crucial role in various renewable energy technologies is by converting mechanical energy into electrical energy or vice versa.

I.2. Definition of renewable energy

Renewable energy sources will play a critical part in the future. The energy resources are classified into three categories: fossil fuels, renewable resources, and nuclear resources[5]. Renewable energy sources are resources that may be utilised to generate energy repeatedly, such as solar energy, wind energy, biomass energy, geothermal energy…etc, and are also known as alternate sources of energy [6]. Renewable energy sources, that satisfy household energy needs, have the ability to deliver energy services with zero or near-zero emissions of both air pollutants and greenhouse gases.

I.3. Different types of renewable resources

Popular renewable energy sources include solar energy, wind energy, hydro energy, tidal energy, geothermal energy, and biomass energy.

I.3.1. Solar energy

Sunlight is one of the most abundant and easily accessible energy sources of our planet. The quantity of solar energy that reaches the earth's surface in one hour exceeds the planet's overall energy requirements for the whole year. Although it appears to be an ideal renewable energy source, the amount of solar energy available depends on the time of day, season, and geographical location.

I.3.2. Wind energy

Wind is an abundant source of renewable energy. Wind farms are becoming more common in the UK, with wind power contributing significantly to the National Grid. Wind turbines are used to operate generators, which subsequently deliver power onto the National Grid. Although residential or 'off-grid' generating solutions are available, not all homes are appropriate for a domestic wind turbine.

I.3.3. Hydro energy

Hydropower is one of the most widely used renewable energy sources. A big reservoir may be utilised to generate power by creating a regulated flow of water via a dam or barrier. This energy source is frequently more dependable than solar or wind power (particularly if tidal rather than river), and it also allows electricity to be stored for use when the demand is high. Hydro, like wind energy, can be more profitable as a commercial energy source in some instances (depending on kind and compared to other sources of energy), but depending on the type of property, it can be utilised for household, 'off-grid' generating.

I.3.4. Geothermal energy

Geothermal energy, which harnesses the natural heat under the earth's surface, may be utilised to directly heat houses or create power.

I.3.5. Biomass energy

This is the process of converting solid fuels derived from plant materials into electricity. Although biomass is primarily about burning organic materials to generate power, it became much cleaner and more energy-efficient process. Biomass creates power at significantly reduced economic and environmental costs by converting agricultural, industrial, and home waste into solid, liquid, and gas fuel [7].

I.4. Photovoltaic system

The photovoltaic system is made up of a power source (photovoltaic generator), a power interface (static converters DC-DC and DC-AC with control system). The static converter's major duty is to create an impedance adjustment so that the generator provides the greatest energy [8].

I.5. Photovoltaic energy

Photovoltaic solar energy is a renewable energy source that converts solar radiation into electricity using photovoltaic cells. A photovoltaic solar panel (or module) is made up of many cells linked together. These are clustered together and termed the photovoltaic field.

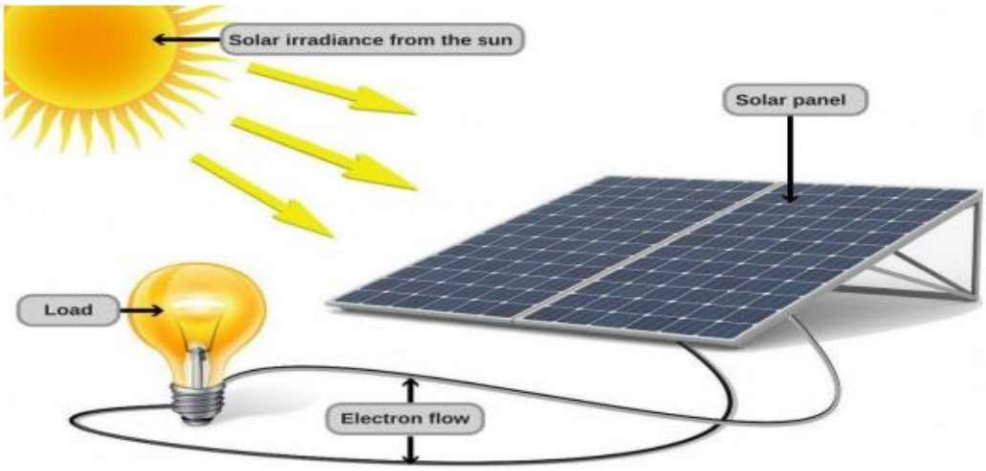

Figure I.1: Photovoltaic solar energy

I.5.1. Solar radiation

Despite the huge distance of 150.10 km between the Sun and the Earth, the Earth's layer gets a significant quantity of energy 180.10 GW, making it an attractive option to other sources. This energy will depart its surface as electromagnetic radiation in a length spanning from 0.22 to 10 µm. The energy associated with this solar radiation is roughly broken down as follows:

- 9% in the ultraviolet band (< 0.4 µm)
- 47% in visible band (0.4 to 0.8 µm)
- 44% in the infrared band (> 0.8 µm) [9].

1.5.2. Photovoltaic effect

The term « photovoltaic » comes from the Greek «photos», which means light and «volta» surname of the Italian physicist (Alessandro Volta) who invented the electric battery in 1800 and gave his name to the unit of measurement of the electric voltage, the volt. In 1905, Einstein discovered that the energy of this quanta of light is proportional to the frequency of the electromagnetic wave.

The photovoltaic effect manifests as a potential difference between the two sides of a semiconductor P-N junction when this junction receives solar radiation of adequate

wavelength and connected to the end with a load. The most widely used industrial material is silicon [10].

I.5.3. Photovoltaic cell

The photovoltaic cell is made of a semiconductor material that absorbs light energy and converts it directly into electricity. The conversion of solar energy into electrical energy is based on the photovoltaic effect, which is the capacity of photons to form load carriers (electrons and holes) in materials. When a semiconductor is illuminated with radiation of the appropriate wavelength, the energy of the absorbed photons allows electronic transitions from the semiconductor's valence band to the conduction band, generating electron-hole pairs that can contribute to current transport when the material is polarized. A PV cell, like a diode used in electronics, can be composed of two layers of silicon, one doped P (boron doped) and the other doped N (phosphorus doped). Between the two zones, a PN junction with a potential barrier emerges. The N zone is covered by a metal grid that acts as a cathode (front contact) and, more importantly, an electron collector, while the opposite side of the crystal is covered by a metal plate (rear contact) that functions as an anode [11].

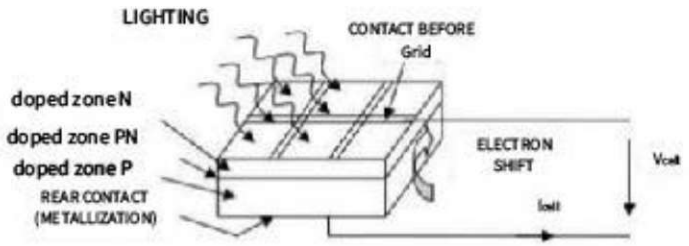

Figure I.2 Principle of operation of the PV cell.

I.6. Different types of photovoltaic cells

There are several varieties of solar cells, often known as photovoltaic cells. Each type of cell has unique efficiency and cost characteristics. However, regardless of the kind, efficiency remains poor, ranging from 8 to 23% of the energy received by the cells. Currently, there are three kinds of cells: monocrystalline, polycrystalline, and amorphous.

- **Monocrystalline cells:** are the photopiles of the first generation, they are made from a block of crystallized silicon in a single crystal, they have a uniform color. They yield

15-22% (See Figure I.3.a).

- **Polycrystalline cells:** are made from a block of crystallized silicon in the form of multiple crystals, they have an efficiency of 11 to 15%, but their production cost is lower than single crystal cells (See Figure I.3.b).
- **Amorphous cells:** are composed of a support in glass or synthetic material on which a thin layer of silicon is arranged (the organization of atoms is no longer regular as in a crystal).

It has the benefit of operating at low illuminance and being more sensitive to high temperatures than mono and polycrystalline cells. However, their output is poor, ranging from 5 to 9% (Figure I.3.c) [12].

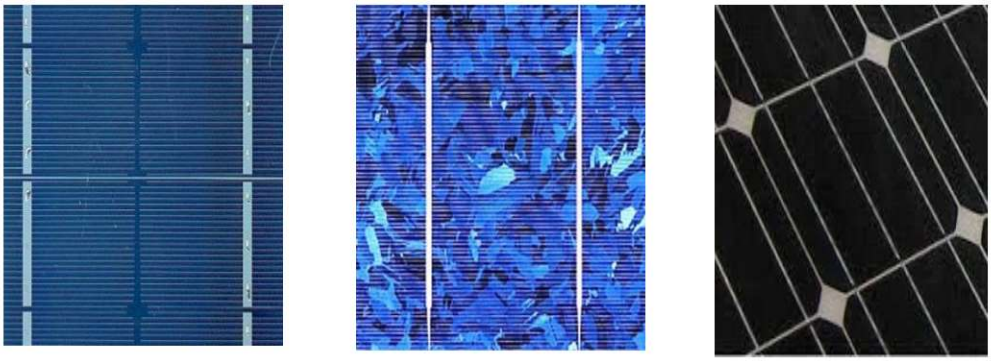

(a) (b) (c)

Figure I.3: Different types of cells [8].

I.6.1. Electrical characteristics of a cell

a. Current / Voltage characteristics

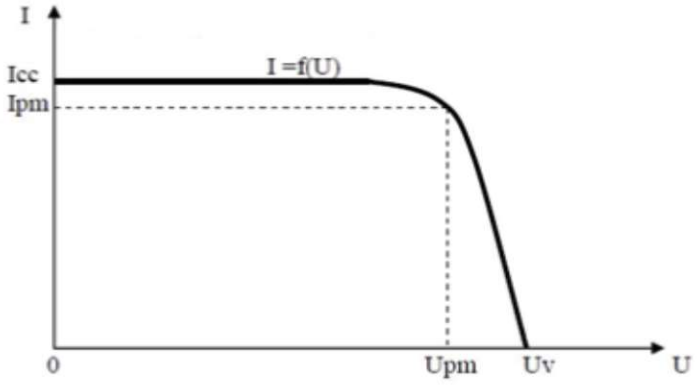

Figure I.4: Characteristic I=f(U) of a photovoltaic cell [13].

On this curve, we find:

- ✓ The vacuum operating point: Uv for I = 0 A
- ✓ The short circuit operating point: Isc for U = 0V

b. Power / Voltage Characteristics:

The power delivered by the cell has for expression P = U.I. For each point of the previous curve, one can calculate the power P and draw the curve P = f(U). This curve has the following appearance:

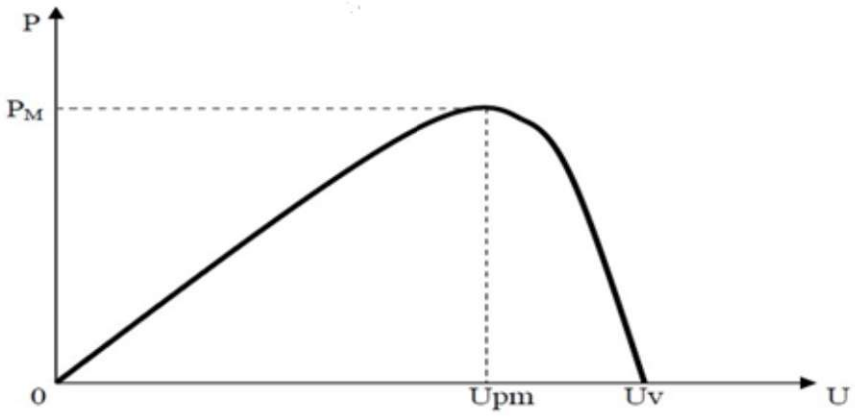

Figure I.5: Characteristic P=f(U) of a photovoltaic cell

This curve goes through a maximum power ($\mathbf{P_M}$). At this power corresponds, an **Upm** voltage and an **Ipm** current that can also be found on the curve I = f(U).

I.7. Photovoltaic module (panel)

A solar cell typically generates less than 2 watts at roughly 0.5 volts. To generate more electricity, the cells are connected to form a module. A solar module (also known as a photovoltaic panel) is formed by connecting numerous cells in series, and a photovoltaic field can be created by connecting many modules in series and/or parallel.

A photovoltaic module is typically made up of a circuit of 36 cells connected in series and sealed with glass and plastic to keep out moisture. The assembly is then fitted with a frame and an electrical junction box.

The transition from a module to a chain (string) is done by the addition of protective diodes, one in series to avoid reverse currents and one in parallel, so-called by-pass diode,

which intervenes only in the event of an imbalance of a set of cells to limit the reverse voltage at the terminals of this set and minimize the associated production loss [14].

I.7.1. Photovoltaic module characteristics

An elementary PV described by the following parameters [15]:

a. **The peak power (Wp):** The nominal power delivered by the module under standard conditions (25°C and an irradiance of 1000 W/m²). It is expressed in peak watts (Wp).
b. **The characteristic I(V):** The curve represents the current (I) flowing through the module as a function of the voltage across it.
c. **The vacuum voltage Voc:** Voltage at the module terminals in the absence of any current, for "full sun" lighting.
d. **The short-circuit current Isc:** Current flow through a short circuit module for "full sun" illumination.
e. **The optimal operating point (The maximum power point – MPP):** It depends on the insolation. This is the point at which the module delivers its maximum current (I_{mpp}) at its maximum voltage (V_{mpp}) when peak power is maximum in full sunlight ($P_{mpp} = V_{mpp} \times I_{mpp}$).

f. **Efficiency:** The ratio of optimal electrical power to incident radiation power. Energy efficiency is defined as the ratio between the maximum power produced (P_{mpp}) and the power of solar radiation reaching the module. Let (S) be the surface area of the module and (G) be the irradiance, this efficiency is expressed as: $\mu = \frac{P_{mpp}}{G*S}$

g. **The form factor :** the ratio of the optimal power (Pmpp) to the maximum power that the module can have.

$$FF = \frac{P_{mpp}}{V_{oc}.I_{sc}} = \frac{V_{mpp} \cdot I_{mpp}}{V_{oc} \cdot I_{sc}} \quad \text{(I.1)}$$

I.8. Photovoltaic field

To produce the required voltage for a load, the panels are linked in series. They then create a string of modules, or string. The chains are then connected in parallel to create a photovoltaic field (PV field).

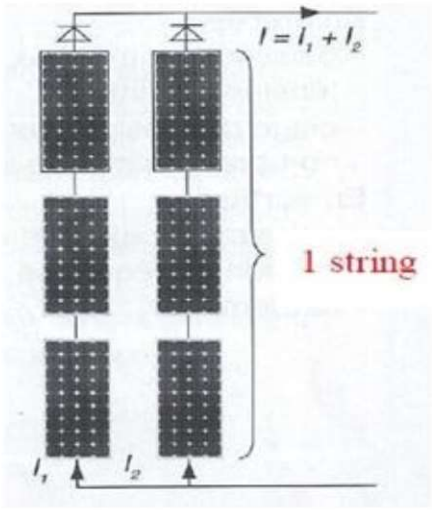

Figure I.6: Two chains of modules constituting a photovoltaic field

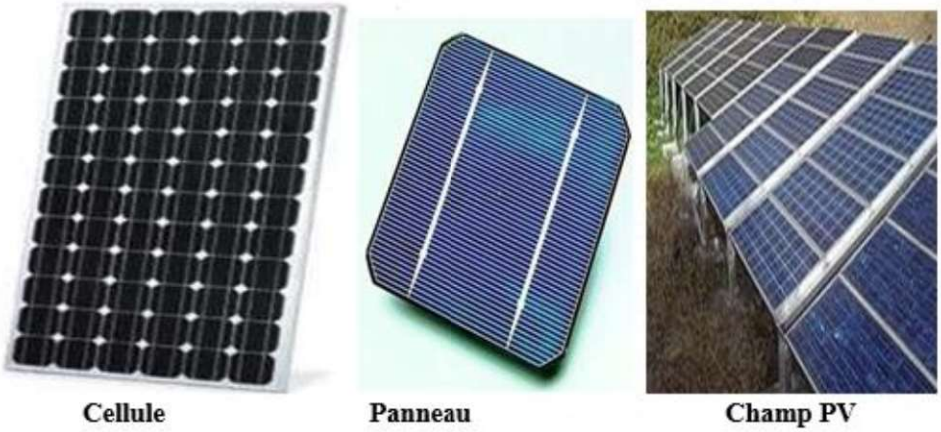

Figure 1.7: Photovoltaic cell, module and field

I.9. Photovoltaic generator

A photovoltaic generator (PVG) is a comprehensive system (series of equipment) that produces and manages power from photovoltaic sensors. The desired application (the nature of the load) determines whether the direct current produced by the PVG is used immediately by the load, stored in batteries, or converted to alternating current using an inverter. The energy is utilized immediately, fed into the grid, or stored in accumulators, so depending on the use.

I.9.1. Grouping modules in a generator

The PVG is generated by combining numerous modules linked either in series or in parallel depending on the demands of the targeted applications.

I.9.2. Serialization

The use of numerous identical modules in series allows for a greater generator V_{GS} output voltage. However, the current remains the same.

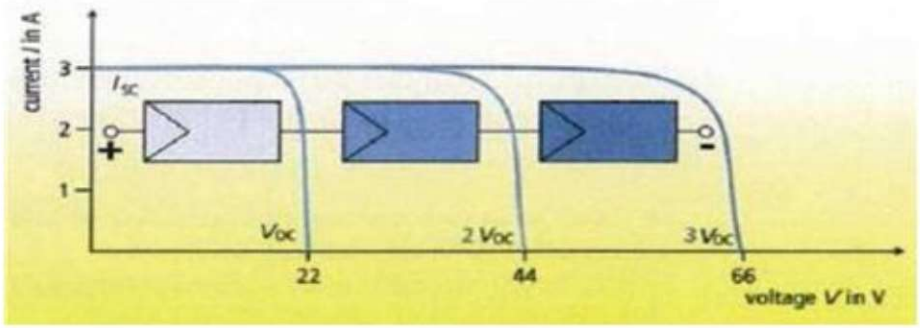

Figure I.8: Characteristic resulting from a grouping of identical modules in series

I.9.3. Parallelization

The grouping of identical modules in parallel allows for a greater generator I_{GS} output current. The voltage remains the same.

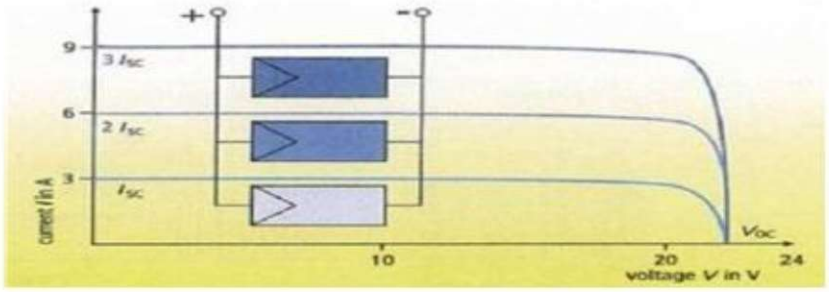

Figure I.9: Characteristic resulting from a grouping of identical modules in parallel [16].

I.10. Standards for connecting photovoltaic systems to the grid

To ensure continuous operation within the specified norms, it is crucial to incorporate key terms such as total harmonic distortion (THD), DC injection, galvanic isolation, detection, and counter-voltage within the appropriate frequency ranges. These elements play a vital role in maintaining the quality and reliability of electrical systems [17].

The most relevant standards, namely IEC 61727 and IEEE 1547-2003, are summarized in Table 1.1. IEC 61727 specifically addresses grid-connected photovoltaic (PV)

systems that utilize semiconductor-based inverters for converting direct current (DC) to alternating current (AC). It provides specific guidelines for systems with a capacity of 10 kVA or less, which are commonly used in single-family homes, whether they operate on a single-phase or three-phase basis. This standard focuses on low-voltage grid connection, as explained in the existing literature [18].

Table I.1: Norms for grid-connected PV systems.

Settings	**IEC 61727**	**IEEE 1547**
THD	< 5 %	< 5 %
Power factor	0.90	0.90
DC current injection	Less than 1% of current nominal output	Less than 0.5% of current nominal output
Voltage range for a normal operation	85 % to 110 %	88 % to 110 %
Frequency range for a normal operation	49 Hz to 51 Hz	59.3 Hz to 60.5 Hz

The IEEE 1547-2003 standard, on its part, offers guidelines for interconnecting distributed energy resources (DER) with the grid. It outlines requirements related to performance, operational procedures, testing, safety considerations, and maintenance of these interconnections [19].

I.10.1. System connected to two-stage network

In a two-stage setup, the conversion process involves two distinct stages. The initial stage employs a DC-DC converter to enhance the generated voltage from the photovoltaic system while tracking the maximum power point. Different types of DC-DC converters, like boost converters, are utilized for this study [20]. The following step involves a DC-AC inverter, which is utilized to manage the DC bus voltage and regulate the current fed into the grid. Two-stage systems provide significant control flexibility in contrast to single-stage setups, as control responsibilities are divided between the two converters. A diagram of a two-stage grid-connected photovoltaic system is illustrated in figure I.10.

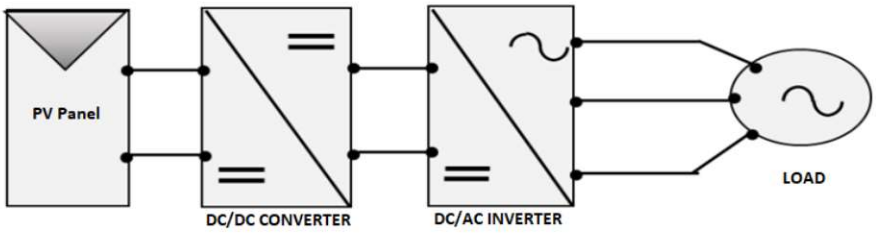

Figure I.10: Diagram of a PV system connected to the two-stage network

I.11. Advantages and disadvantages

I.11.1. Advantages

- ✓ High reliability: it does not have moving parts that make it particularly suitable for remote areas. This is the reason for its use on spacecraft.
- ✓ The modular nature of the photovoltaic panels allows a simple and adaptable assembly to various energy needs.
- ✓ Their operating costs are very low given the reduced maintenance.
- ✓ It is not a source of pollution, is quiet, and does not disturb the environment.

I.11.2. Disadvantages

- ✓ The manufacture of the photovoltaic module is high technology and requires high-cost investments.
- ✓ A module has low conversion efficiency.
- ✓ Photovoltaic generators are only competitive with diesel generators for low energy demands in remote areas.
- ✓ Tributaire des conditions météorologiques [21].

I.12. Electromechanical system

Electromechanical system consists of three subsystems, each with specific properties that enable various functions based on the desired trajectory for the device. In Figure I.11, we can see the blocks representing these modules, each highlighted for its distinct characteristics.

The electric circuit plays a crucial role in controlling the electromechanical system when it functions as an electric motor. Similarly, when the device operates as a generator, the electric circuit becomes essential to ensure that the generated output voltage aligns with the requirements of the load or the power system.

A typical equation system of the electric circuit connected to the electromechanical device is:

$$V_i = r_i i_i + L_i \frac{di_i}{dt} + e_i(t); i = 1,2 \dots m \quad (I.2)$$

In motor operation, the mechanical subsystem is characterized by force or torque balance equations. Conversely, in generator operation, it is described by prime mover equations.

A typical equation system for a translational movement issuing from the mechanical subsystem is given by:

$$F_{mec} - F_{mag} = m\frac{dv}{dt} + Kv + c\int_{t0}^{t} vdt \quad (I.3)$$

For a rotating electromechanical system, we have:

$$T_{mec} - T_{mag} = J\frac{d\omega}{dt} + K\omega + c\int_{t0}^{t} \omega dt \quad (I.4)$$

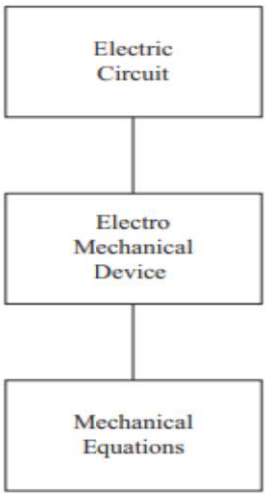

Figure I.11: Flow chart of electromechanical device analysis.

Where:

m: mass of the moving parts

K: damping constant

C: spring constant

J: moment of inertia

The block diagram of the electromechanical device incorporates equations that connect both the electric circuit and mechanical subsystems. Consequently, the equations of the electromechanical device encompass values from both the electric and mechanical components. Due to the typically non-complex geometries of ordinary electromechanical devices, the laws of electromagnetism, which involve electromotive force and force (or torque), are relatively straightforward [22].

I.13. Electromechanical energy conversion

Electromechanical energy conversion entails the transformation of mechanical energy into electrical energy (in generators) or the reverse process (in motors), utilizing rotary motion (in rotary machines) or translatory motion (in linear machines and actuators). These conversion devices are commonly referred to as electrical machines, solenoid actuators, and electromagnets.

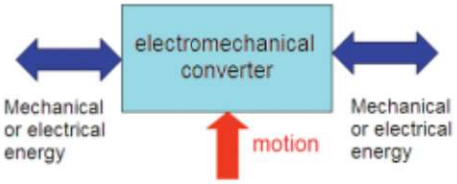

Figure I.12: Electromechanical energy conversion.

Transformers and solid-state converters are not categorized as electromechanical energy conversion devices because they solely alter one form of electrical energy into another form with varying parameters (such as voltage, current, frequency, and number of phases, conversion between AC and DC) without involving any mechanical motion.

I.13.1. Application of electromechanical system

An example of application of an electric motor is shown in Figure I.13, and an example of application of an electric generator is shown in Figure I.14. It means that the input is an electrical energy and, in the output, we have mechanical energy while in the second example we have vice versa.

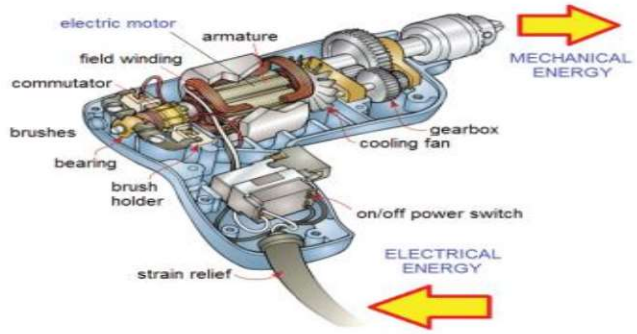

Figure I.13: Power tool: an example of conversion of electrical energy into mechanical energy.

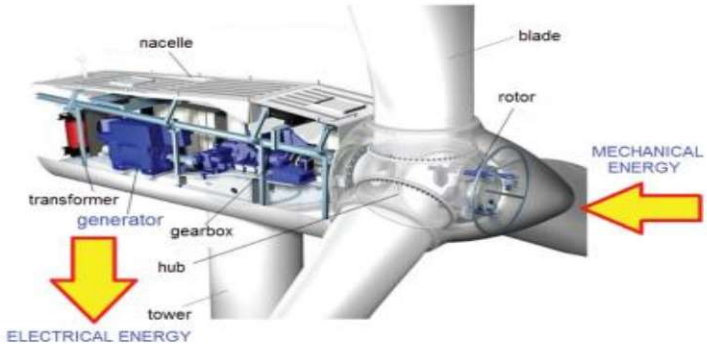

Figure I.14: Wind turbine generator: an example of conversion of mechanical energy into electrical energy

I.13.2. Energy flows in an electromechanical energy conversion device

Figure I.15 illustrates the conversion of electrical energy into mechanical energy, with the following breakdown:

$$dW_e = dW_f + dW_{loss} + dW_{mech} \quad (I.5)$$

Where:

- dW_e represents the electrical energy (input energy).
- dW_f denotes the energy stored in the magnetic field (coil).
- dW_{loss} accounts for all power losses.
- dW_{mech} signifies the mechanical energy (output energy).

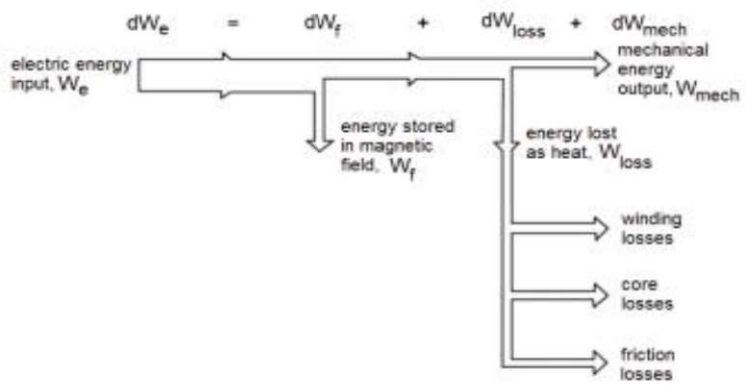

Figure I.15: Energy flows in electromechanical energy conversion device.

Table I.2: Analogies in electric and magnetic circuits

Quantity	Electric circuit	Magnetic circuit
Voltage	Electric voltage, V [V]	Magnetic voltage drop,V_μ[A]
Source voltage	Elctromotive force (EMF), E[V]	Magnetomotive force (MMF), F[A]
Current / flux	Electric current, I[A]	Magnetic flux, Φ[Wb]
Resistance / reluctance	Resistance R[Ω=[1/S]]	Reluctance $R_\mu[1/\mathrm{H}]$
Constant	Electric conductivity,$\sigma[\mathrm{S/m}]$	Magnetic permeability, μ[H/m]

Table I.3: Comparison of fundamental laws for electric and magnetic circuits [23].

Law	Electric circuit	Magnetic circuit
Ohm's law	Resistance $R = \frac{V}{T}$ Conductance $G = \frac{I}{V}$	Reluctance $R_\mu = \frac{V_\mu}{\phi}$ Permeance $A_\mu = \frac{\phi}{V_\mu}$
2nd Ohm's law	Resistance $R = \frac{I}{\sigma t}$ Conductance $G = \frac{S}{\rho t}$	Reluctance$R_\mu = \frac{l}{\mu S}$ Permeance$A_\mu = \frac{\mu S}{l}$
Kirchhoff's current law	Sum of currents $\sum I = 0$	Sum of magnetic fluxes $\sum \phi = 0$
Kirchhoff's voltage law	Sum of voltage drops $\sum V - \sum RI = 0$	Sum of magnetic voltage drops $\sum V_\mu - \sum R_\mu \phi = 0$
Faraday's law/ Ampere's law	EMF $E = \pi\sqrt{2} f N \phi$	MMF F=NI

I.14. Main components of the electromechanical system

Electromechanical assembly generally requires multiple processes. Initially, the mechanical components of the system are developed and constructed. These components might range from gears and bearings to actuators and structural supports. Electrical components are also developed and built independently, and may comprise wire, sensors, and control modules. When the individual components are finished, they are combined into a complete system. This is usually performed by connecting the electrical components and merging them with the mechanical ones. Depending on the complexity of the system and the resources available, the process may need both manual work and automated activities.

Electromechanical assembly is an essential part of many industries since it allows for the creation of complex systems capable of serving a number of functions. Electromechanical assembly, for example, is used in the automobile industry to create complex systems that control the engine, transmission, and brake systems. Similarly, in the aerospace sector, electromechanical assembly is used to construct intricate systems such as rocket and satellite navigation and control systems [24].

I.14.1. Asynchronous machine

The asynchronous motor is the most widely used machine in the field of powers greater than a few kilowatts because it has many advantages such as its power-to-weight ratio, robustness, ease of implementation, low cost, etc. The emergence in the 1980s of variable speed drives allowing the rotation frequency to be varied over a wide range greatly favored its development. Indeed, it is used in the design of numerous industrial processes combining static converters and electric machines (electric traction, rolling mills, lifting, pumping, etc.). Although the asynchronous machine has the reputation of being robust, like any other electric machine, it can present electrical or mechanical failures. Thus, due to the significant and costly consequences that the appearance of a fault can entail on industrial processes, fault diagnosis has been the subject of considerable interest over the past two decades.

The electromagnetic interaction of the two parts of the machine is only possible when the speed of the rotating field (n_1) differs from that of the rotor (n), i.e., when $n \neq n_1$, because otherwise, when $n = n_1$, the field would be stationary relative to the rotor and no current would be induced in the rotor winding. The ratio $g = \frac{n1-n}{n1}$ is called the slip of the asynchronous machine [25].

I.15. Power converter

Power converters are a type of electrical circuit that converts electrical energy from one level of voltage, current, or frequency to other utilising semiconductor electronic switches. They are critical components in electronic and electrical systems.

Power converters operate by changing the electrical properties from one form to another to meet the needs of certain devices or systems. Power converters use a range of electrical components and processes that are specific to the kind of conversion (AC-DC, DC-AC, DC-DC, or AC-AC). Although there are numerous types of power converters, they are all built of the same basic components:

- Diodes and thyristors allow current to flow in one direction.
- Inverters and DC-DC converters use transistors and MOSFETs to switch quickly.
- Capacitors and inductors store and filter energy, smoothing down voltage and current waveforms.
- Microcontrollers control switches to create desired outputs.

I.15.1. Different power converter types

A variety of power converters are available to meet the specific needs of a given application.

- **AC-DC converters (rectifiers)** these converters convert alternating current (AC) from the power grid into direct current (DC), which is required by most modern equipment. They are often found in a variety of power supply, such as battery chargers and electrical devices.
- **DC-AC converters** often called inverters. These convert DC electricity (derived from batteries or solar panels) into AC power, which may then be utilised to power AC equipment or sent into the power grid. They are critical components in renewable energy systems, portable power systems, and backup power sources.
- **DC-DC converters** are used to convert DC electricity from one voltage level to another. This is critical in electronics, as various components require varying voltage levels. They are commonly employed in battery-powered gadgets, laptop computers, and automotive power management systems. There are different types of DC-DC converters, including :
  - **Buck converters**, it reduces voltage from a higher to a lower level.

- **Boost converters**, it increases voltage from a lower to a greater level.
- **Buck-boost**, this might increase or decrease the voltage.
- **Isolated converters**, which contain transformers to provide electrical isolation between the input and output, with variations such as the flyback, forward, and push-pull converters.

➢ **AC-AC converters** convert one type of AC power (at a given voltage and frequency) into another. They may adjust the output frequency and voltage and are helpful in applications requiring frequency conversion (for example, from 60Hz to 50Hz) or variable frequency drives to control the speed of AC motors. AC-AC converters are available in a variety of configurations, similar to DC-DC converters:

- Cycloconverters transform the incoming energy into a lower frequency alternating current output.
- AC voltage controllers modify the input waveform to manage the RMS voltage delivered to the load [26].

I.16. Flywheel

Generating electricity through conventional methods demands a substantial energy input, often derived from fuels that undergo transformation into various energy forms. Modern power generation employs integrated motor-generator systems, where electric energy propels a mass. This contemporary approach involves the conversion of multiple energy types. For example, a motor can be employed to rotate a spinning mass, leveraging its inertia to sustain motion. This rotational energy from the spinning mass, referred to as a flywheel, is subsequently utilized to drive the alternator and generate electricity.

Our study aims to harness free energy using a flywheel. By employing a gear train comprising a series of belt and pulley drives, connected to a main motor with a capacity of one and a half horsepower, the shaft of an alternator rotates more than twice as fast. This system is intriguing because it seemingly generates more electrical output power from the alternator than what is expected from the input motor. The flywheel plays a crucial role in this setup. To maximize the production of additional or free energy, the gear train is integrated with the flywheel or gravity wheel. A comprehensive analysis of the various properties of the flywheel is conducted to optimize the extraction of free energy from the system.

I.16.1. Materials and methods

I.16.1.1 Materials

- **Flywheel**: Indeed, a flywheel functions as a reservoir for energy, accumulating excess energy when the supply exceeds demand and releasing it when demand surpasses supply. This stored energy within the flywheel manifests as kinetic energy. Utilizing belt drives, this amassed kinetic energy is transferred to drive the alternator, thereby generating electricity.

(a) **(b)**

Figure I.16: a) Automobile flywheel. b) Conventional flywheel

- **Pulley**: Pulleys guide cables and change the direction of pulling force, aiding in lifting heavy objects with less effort through mechanical advantage.
- **Belt**: Belts are flexible loops connecting spinning shafts, running parallel. They provide motion, transmit power, or track relative movement. When looped over pulleys, shafts don't have to be parallel, there can be a twist. In a two-pulley system, belts can reverse or maintain direction. Different pulley sizes adjust rotational speed.

Figure I.17 : Belt and Pully

- **Shaft**: A shaft is a rotati ransfers power from one part to another, often utilizing transmission elements such as pulleys and gears.
- **Bearing**: A bearing is a vital component of a machine designed to restrict relative motion to only essential movement and reduce friction between moving parts.
- **Motor/ Generator**: flywheels are intricate devices designed to store and release energy efficiently. They typically involve electrical machinery such as motors and generators to accomplish this task. These components function both as motors, driving

the flywheel to store energy, and as generators, extracting stored energy from the flywheel to produce electrical energy. This dual functionality allows for the efficient storage and retrieval of energy within the flywheel system, making it a versatile solution for various applications requiring energy management and stabilization.

I.16.1.2. Methods

- Flywheels have a rich history spanning thousands of years, but in modern times, internal combustion engines have predominantly dominated. Acting as a simple yet effective mechanical energy reservoir, a flywheel operates by storing energy within a rotating disc as it spins around its axis. The amount of stored energy is proportionate to the square of the rotational speed and the mass of the object, demonstrating an inverse relationship.
- Kinetic storage, also known as FES (Flywheel Energy Storage), encompasses a broad concept utilized across various technical fields. Central to this system is an integrated motor-generator housed within a unit, which is interconnected with the flywheel rotors. The kinetic energy generated by the rotating flywheel is harnessed and subsequently stored by the motor-generator mechanism. Implementing a flywheel power system offers several advantages including prolonging battery life, obviating the necessity for batteries altogether, fostering energy sustainability, and facilitating power frequency control [27].

I.18. Conclusion

This chapter allowed us to give a general overview on renewable energies and especially the photovoltaic system. Generalities have given on the various renewable energies and photovoltaic solar system with a description of the PV cell, the basic element of photonic-electric conversion, the PV module, the PV field and the PVG. The second part of the chapter is devoted to the PV generator and their characteristics I(V) and P(V). In the next chapter, we will present a study of an electromechanical system for electric power production, based on a PVG, an asynchronous motor, a flywheel, and a synchronous generator.

Overall, electromechanical assembly is a critical process in many industries, allowing for the creation of complex systems that combine both electrical and mechanical components. While the process can be complex and challenging, it offers a high degree of flexibility and customisation, making it a valuable tool for manufacturers and engineers.

Chapter II
Modeling of the association PV-Electromechanical system

II.1. Introduction

A photovoltaic system consists of various components that make up the production source, represented by the photovoltaic generator (PVG), which converts solar energy into electrical energy. It includes static converters (such as a chopper and an inverter) to adjust the system and ensure maximum power point, and the load, which consumes and utilizes the power provided by the PVG.

This chapter aims to model the photovoltaic system by providing an illustration of each element. We will present the mathematical model of the whole system, which from PVG to synchrone generator. We will discuss the principle of Maximum Power Point Tracking (MPPT) control to find the point where the power delivered by the PVG to the asynchronous motor is maximum.

II.2. Overview of the system

Our representative system consists of:

- **Photovoltaic Generator:** Based on an STPO80-12/Bb module consisting of 36 monocrystalline silicon cells connected in series with a maximum power of 80 W.
- **Boost Converter:** The boost converter elevates the output voltage of the PV generator and is equipped with MPPT control, enabling the pursuit of maximum power point, based on the Perturb & Observe (P&O) method.
- **Inverter**: The three-phase voltage inverter with Metal Oxide Semiconductor Field Effect Transistor (MOSFET) operates based on the sinusoidal-triangle method for generating control pulses for the MOSFETs using Pulse Width Modulation (PWM).
- **Asynchronous Motor:** The system drive actuator is represented by the squirrel-cage asynchronous motor.

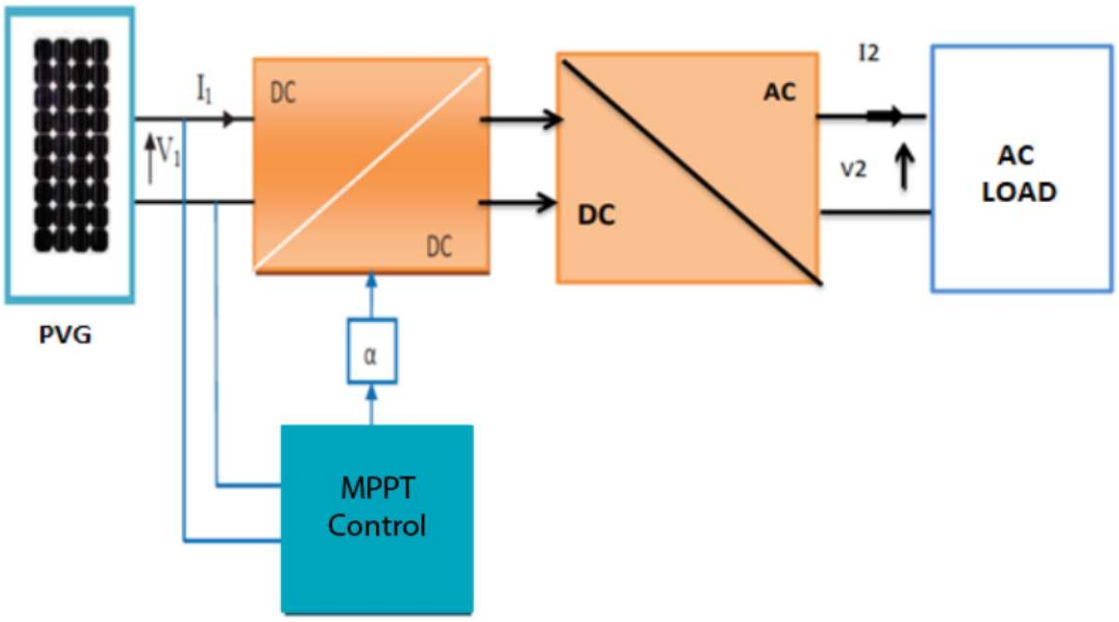

Figure II.1: Elementary Photovoltaic Conversion Chain

II.3. PV cells modeling

It requires a judicious choice of equivalent electrical circuits. To develop an accurate equivalent circuit for a PV cell, it is necessary to understand the physical configuration of the cell's elements as well as the electrical characteristics of each element. Following this philosophy, several electrical models have been proposed to represent the photovoltaic cell. These models differ in their mathematical procedures and the number of parameters involved in calculating the voltage and current of the PV module [8].

Among these models, the following can be cited:

- Single diode model (one exponential)
- Two-diode model (two exponentials)

In our study, we have chosen the single diode model.

II.3.1. Single Diode Model

This is the most classical and widely used model in the literature, developed by Eck Stein (1990). This model takes into account physical phenomena. It involves a current generator for modeling the light flux, a diode for junction polarization phenomena, and two resistances (series and shunt) for losses [28].

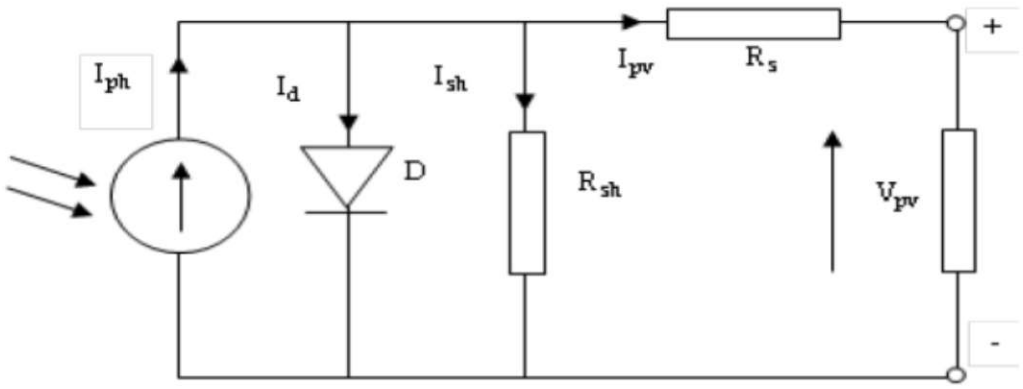

Figure II.2: Model of a PV Cell as a Diode

This model has the advantage of being simple, allowing to obtain the static behavior of a PV cell under polarization.

$$Ipv = Iph - Id - Ish \tag{II.1}$$

Where :

- Ipv : represents the current of the PV cell,
- Iph: is the photocurrent, proportional to the illumination,
- Id: is the current flowing through the ideal diode D (which models the junction in parallel),
- Ish: is the current flowing through the shunt resistance.

II.3.2. Characteristic equations of a photovoltaic cell

There are several ways to present and calculate the current of a PV cell (Eq. II.1). To do this, we have chosen a simplified and improved mathematical model [29], [30]. The I-V characteristic can be written as follows:

$$Ipv = Iph - I0\left[\exp\left(\frac{Vpv + Rs.Ipv}{Vt}\right) - 1\right] - \left(\frac{Vpv + Rs.Ipv}{Rsh}\right) \tag{II.2}$$

And for a module, the number of cells in series is taken into consideration:

$$\mathrm{I}mpv = Iph - I0\left[\exp\left(\frac{Vpv + Rs.Ipv}{Ns.Vt}\right) - 1\right] - \left(\frac{Vpv + Rs.Ipv}{Rsh}\right) \tag{II.3}$$

With:

Vt: thermal voltage (V).

Ns: number of cells in series.

Io: saturation current. It depends on the junction temperature (A).

Rs: series resistance, which represents various resistances of metallic contacts and connections. It is very low (Ω).

Rsh: shunt resistance (much higher compared to Rs). A low Rsh, will have an impact on the open-circuit voltage. It characterizes the leakage current at the junction (Ω).

Generally, the resistance values are given as follows:

$$Rsh > 100\frac{Voc}{Isc} \qquad \text{And} \qquad Rs < 0.01\frac{Voc}{Isc}$$

The photon current is given by:

$$Iph = Iscn + Ki\left(T - Tn\right)\frac{G}{Gn} \tag{II.4}$$

With:

$Iscn$: nominal short-circuit current (A)

Ki: temperature coefficient of short-circuit current (A/K) or (A/°C)

T: operating temperature (K)

Tn: nominal temperature (298 K)

Gn: irradiance under standard conditions (Gn =1000W/m^2)

The saturation current is given by:

$$Io = \frac{Iph}{e(\frac{Voc}{Vt.Ns}) - 1} \tag{II.5}$$

With:

Voc : the open-circuit voltage

Vt : the thermal voltage

The open-circuit voltage is given by the formula below:

$$Voc = Kv(T - Tn) + Vocn \quad \text{(II.6)}$$

Where:

Kv: the coefficient of temperature for open-circuit voltage (V/K) or (V/°C)

$Vocn$: the nominal open-circuit voltage (V)

And the thermal voltage is given by the following relationship:

$$Vt = \frac{a(T - T0)K}{q} = \frac{aK(T)}{q} \quad \text{(II.7)}$$

With:

a: the ideality factor of the junction, ranging between 1 and 2.

K: the Boltzmann constant is equal to 1.38 × 1 0 − 23 (J/K)

q: the charge of an electron (q = 1.6 × 10−^{19}C)

T: the operating temperature in Kelvin (K), and T 0 = 273 K.

The equation for the voltage-current characteristic of a PV array:

$$\mathrm{I} = Npp.Iph - Npp.Io\left[\exp\left(\frac{Vpv + (\frac{Rs.Nss}{Npp}).Ipv}{Ns.Vt}\right) - 1\right] - \left(\frac{Vpv + (\frac{Rs.Nss}{Npp}).Ipv}{Rp(\frac{Nss}{Npp})}\right) \quad \text{(II.8)}$$

Npp: the number of modules in parallel.

Nss: the number of modules in series.

III.4. DC/DC Converter

It is a boost converter implementing one or more controlled switches, allowing modifying the voltage of a DC voltage source with high efficiency.

There are three types of DC/DC converter:

- Step-down chopper (Buck or series): the average output voltage is lower than the applied input voltage.
- Step-up chopper (Boost or parallel): the average output voltage is higher than the applied input voltage.

- Step-down/Step-up chopper (Buck-Boost or series-parallel): these choppers are capable of operating in two ways (Buck-Boost), where the average output voltage is either lower or higher than that of the input.

In our study, the Boost converter is used as a load adapter, enabling the pursuit of the maximum power point [11].

II.4.1. Boost Converter

A boost converter, also known as a step-up converter, allows converting a DC input voltage into another DC output voltage that is higher than the input voltage. This is why it's called a voltage booster [16].

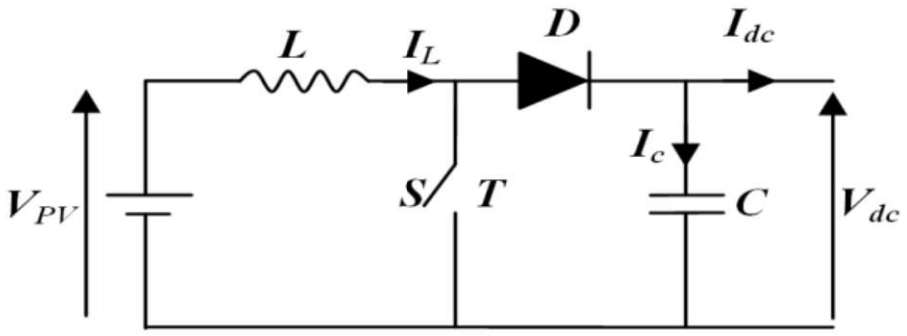

Figure II.3: Electrical circuit of the boost converter

The inductance serves to smooth the current drawn from the source, while the capacitance (*C)* aims to limit the voltage ripple at the output. Its operation is as follows:

At the initial time (αT), the switch (*S*) is closed, allowing the current in the inductance to gradually increase. As time progresses, it stores energy until the end of the first period. When the switch opens, the inductance (*L*) resists the decrease in current (I_L), generating a voltage that adds to the source voltage. This voltage is then applied to the load through the diode (*D*).

II.5. Boost converter modeling

The modeling of this converter is based on the analysis of different operating sequences, which we will assume have durations fixed by the control *S*. (See Figure II.3). As a result, we have two operating sequences depending on the state of the switch *T*, each of which can be represented by a differential equation [16], [31].

- When (T) is closed:

$$V_{pv} = L\frac{dI_L}{dt} \quad \text{(II.9)}$$

$$0 = c\frac{dV_{dc}}{dt} + I_{dc} \quad \text{(II.10)}$$

- When (T) is open :

$$V_{pv} = L\frac{dI_L}{dt} + V_{dc} \quad \text{(II.11)}$$

$$I_L = c\frac{dV_{dc}}{dt} + I_{dc} \quad \text{(II.12)}$$

By defining:

(S= 1) for when T is closed

(S= 0) for when T is open.

We can represent the converter by a single system of equations, which we refer to as an instantaneous model. Here, we consider ideal switches.

$$V_{pv} = L\frac{dI_L}{dt} + V_{dc}(1 - S) \quad \text{(II.13)}$$

$$(1 - S)I_L = c\frac{dV_{dc}}{dt} + I_{dc} \quad \text{(II.14)}$$

II.6. Power maximization command

The pursuit of Maximum Power Point Tracking (MPPT) allows the photovoltaic generator to deliver its maximum power. The tracker is typically designed with a converter using an appropriate control technique, such as a boost converter. These techniques are generally classified into two categories: indirect methods and direct methods. The latter are typically represented by the Perturbation & Observation method (P&O) and the Incremental Conductance method. In this case, we opted for the P&O method because it is very easy to implement and offers good performance.

II.7. Perturbation and Observation method

The P&O algorithm, which is the most widely used for MPPT, operates by perturbing the system. This is done by increasing or decreasing V_{ref} or directly modifying the duty cycle of the DC/DC converter, and then observing the effect on the output power of the panel. If the current power value P(k) of the panel is greater than the previous value P(k−1), the same

direction of perturbation is maintained, otherwise, the perturbation is reversed from the previous cycle.

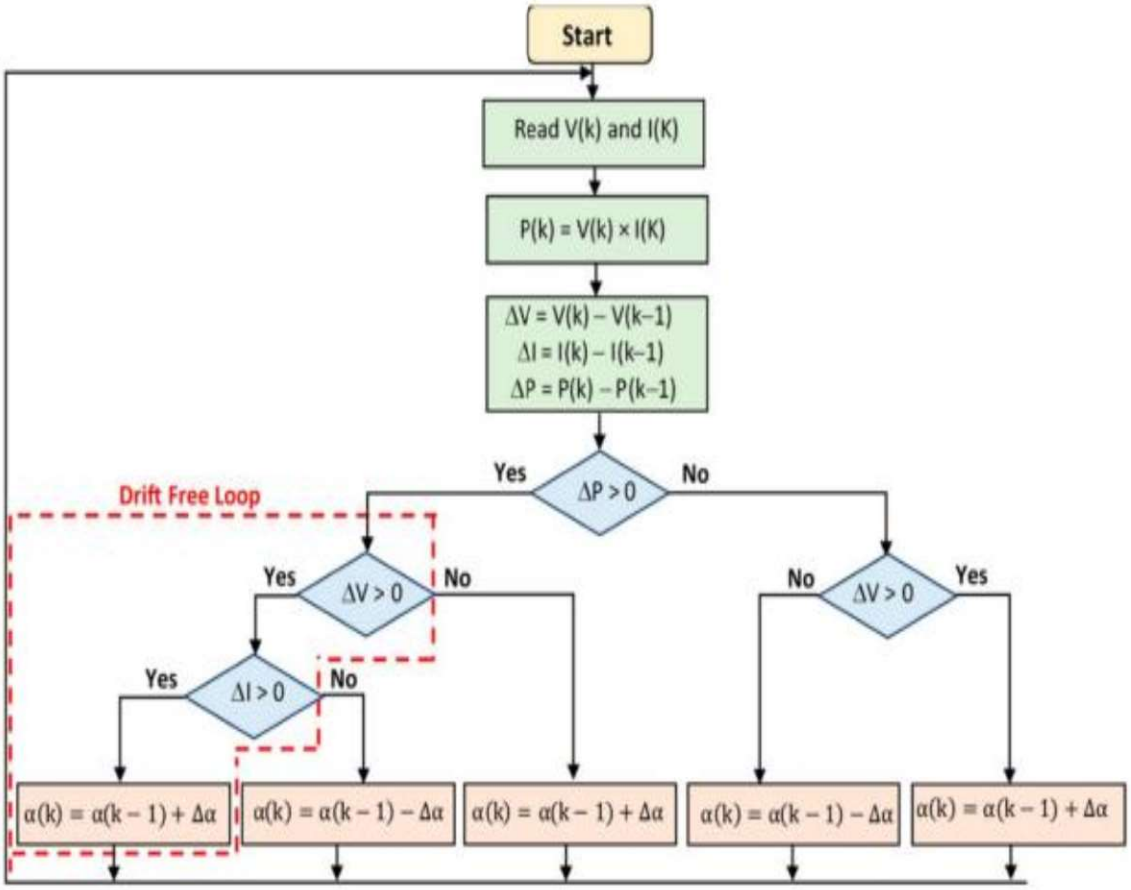

Figure II.4: Algorithm's Organizational Chart

With:

Cp: the step size of a single perturbation.

First, the voltage V and current I are measured to calculate the P(k). This value is compared to the power value obtained during the last measurement (k−1).

- If the power supplied by the panel has increased since the last measurement, the increment or decrements of the duty cycle α will continue in the same direction as in the last cycle, which is determined by testing dV, where:

If dV >0; this means V was increased during the last cycle.

$$(k+1) = (k) + \Delta\alpha \qquad \text{(II.15)}$$

If dV <0; this means V was decreased during the last cycle.

$$(k+1) = (k) - \Delta\alpha \quad \text{(II.16)}$$

Thus, the algorithm continues in the direction where P continues to increase.

- If the power supplied by the panel has decreased since the last measurement, the increment of the duty cycle α will be in the opposite direction to the last cycle, also determined by testing dV. With this algorithm, the operating voltage V is perturbed with each cycle [8].

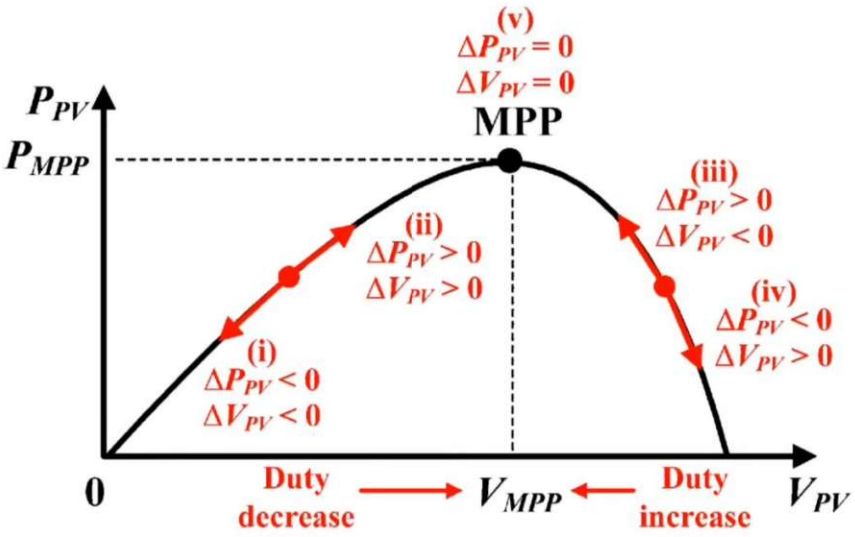

Figure II.5: schematic converge to MPP by P&O

II.8. DC/AC Converter

The output voltage waveform of the inverter should closely resemble a sine wave, meaning the harmonic distortion should be very low, which primarily depends on the control technique used. In the system where an asynchronous motor is powered by a PVG, the direct current provided needs to be converted into alternating current to power the motor. In this context, a three-phase voltage inverter is required.

II.9. Modeling of the inverter

The two-level three-phase voltage inverter consists of a DC voltage source and six switches arranged in a bridge configuration. The DC voltage is obtained through a boost converter. To obtain an alternating voltage from a direct voltage, the input voltage needs to be chopped and applied to the load in both directions. The operating frequency is set by the switch control. The inverter assembly comprises six bidirectional switches. The pairs of

switches in each leg are controlled in a complementary manner to ensure the continuity of currents in the static phases of the asynchronous machine and to prevent short-circuiting of the source. Each switch consists of a transistor (T) and a diode (D) arranged in a head-to-toe configuration, figure II.6 [32].

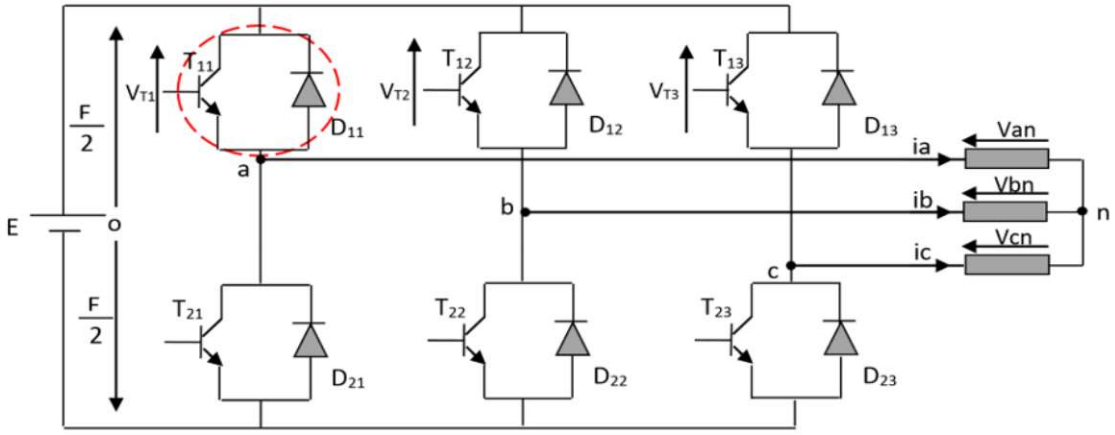

Figure II.6: Diagram of the three-phase inverter.

To simplify the study and the complexity of the inverter's structure, we will assume that:

- Switching between the interconnectors happens instantly. Switching between the interconnectors happens instantly.
- The voltage drop across the switches is negligible.
- The three-phase load is balanced and star-connected.

Given that in a balanced system $v_{an}+v_{bn}+v_{cn}=0$, we can write, as shown in Figure II.6:

$$\begin{cases} v_{an} = v_{ao} + v_{on} \\ v_{bn} = v_{bo} + v_{on} \\ v_{cn} = v_{co} + v_{on} \end{cases} \quad \text{(II.17)}$$

By summing the equations of system (III.12), we obtain:

$$V_{an} + V_{bn} + V_{cn} = V_{ao} + V_{bo} + V_{co} + 3V_{on} = 0 \quad \text{(II.18)}$$

Where :

$$V_{ao} + V_{bo} + V_{co} = -3V_{on} \quad \text{(II.19)}$$

Therefore :

$$V_{on} = -1/3(V_{ao} + V_{bo} + V_{co}) \tag{II.20}$$

By substituting equation (II.15) into system (II.12), we then have:

$$\begin{bmatrix} V_{an} \\ V_{bn} \\ V_{cn} \end{bmatrix} = \frac{1}{3} \begin{bmatrix} 2 & -1 & -1 \\ -1 & 2 & -1 \\ -1 & -1 & 2 \end{bmatrix} \begin{bmatrix} V_{ao} \\ V_{bo} \\ V_{co} \end{bmatrix} \tag{II.21}$$

According to the condition of the static switches (S_k) of the inverter (S_k is equal to 1 if the switch is closed and 0 if not, with k=a),

$$S_k = 1 \quad \text{Otherwise} \quad S_K = 0$$

$$V_{ko} = (2V_k - 1).E/2 \tag{II.22}$$

After simplification, the mathematical model of the two-level voltage inverter is given by equation II.18.

$$\begin{bmatrix} V_{an} \\ V_{bn} \\ V_{cn} \end{bmatrix} = \frac{E}{3} \begin{bmatrix} 2 & -1 & -1 \\ -1 & 2 & -1 \\ -1 & -1 & 2 \end{bmatrix} \begin{bmatrix} S_a \\ S_b \\ S_c \end{bmatrix} \tag{II.23}$$

II.10. Sinusoidal Pulse Width Modulation

The sinusoidal pulse width modulation is achieved by comparing a low-frequency modulating signal (reference voltage) with a high-frequency triangular carrier waveform. The switching instants are determined by the intersections between the carrier and the modulating signal, and the switching frequency of the switches is determined by the carrier frequency. In three-phase systems, three sinusoidal references, phase-shifted by 2π/3 at the same frequency fs [34].

This describes a sinusoidal modulating signal with amplitude A_r and frequency f_r combined with a high-frequency triangular carrier signal with amplitude A_p and frequency f_p. The switching angles of the input voltage of a bridge are located at the intersections of the carrier and the modulating signal (Figure II.7).

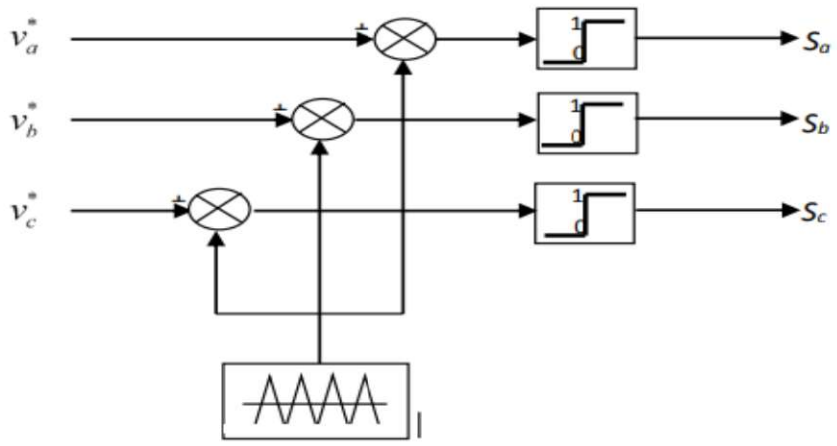

Figure II.7: Principle of PWM

The sinusoidal reference voltages are expressed as follows:

$$V_a = V_m \sin(\omega t)$$

$$V_b = V_m \sin(\omega t - \frac{2\pi}{3}) \quad \text{(II.24)}$$

$$V_c = V_m \sin(\omega t - \frac{4\pi}{3})$$

The equation of the triangular carrier waveform is expressed as follows:

$$V_p(t) = \begin{cases} V_{pm}\left[4\left(\frac{t}{T_P}\right) - 1\right] - 1 & if \quad 0 \le t \le \frac{T_P}{2} \\ V_{pm}\left[-4\left(\frac{t}{T_P}\right) + 3\right] + 3 & if \quad \frac{T_P}{2} \le t \le T_P \end{cases} \quad \text{(II.25)}$$

The sinusoidal pulse width modulation (SPWM) control uses comparison with the carrier waveform of the three components of the reference voltage to calculate the states a, b, and c of the inverter switches. These are given by the following equation :

$$V_p(t) = \begin{cases} 1 & if \quad \left((V_{rabc} - x(t)\right) \ge 0 \\ 0 & if \quad \left((V_{rabc} - x(t)\right) < 0 \end{cases} \quad \text{(II.26)}$$

This technique is characterized by the following two parameters:

- Modulation index (m) equal to the ratio of the modulation frequency (f_P) to the reference frequency (f_r), ($m = \frac{f_P}{f_r}$).

- Modulation rate (r) equal to the ratio of the amplitude of the reference voltage (V_r) to the peak value of the modulation waveform (V_p), ($r = \frac{V_r}{V_p}$).

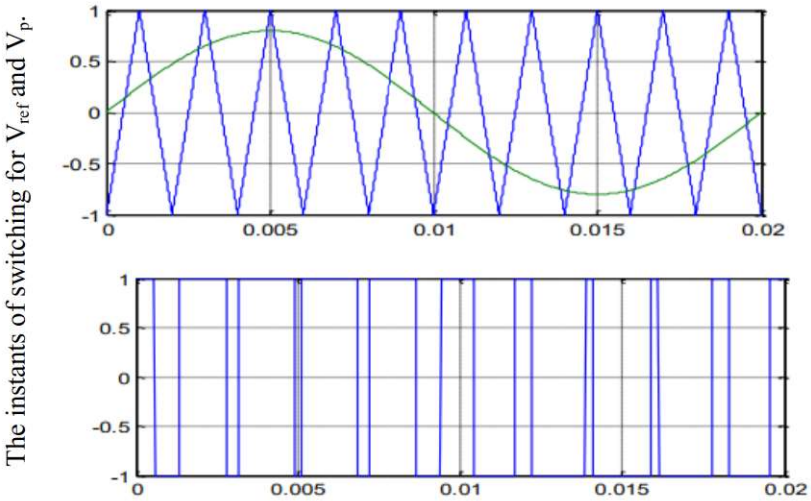

Figure II.8: Description of Pulse Width Modulation (PWM).

II.11. Asynchronous motor Modeling

Before presenting the modeling of the asynchronous motor (ASM), and to simplify the model, we made the following simplifying assumptions [31-33], [35]:

- Magnetic circuit saturation is negligible.
- Hysteresis and eddy current losses are neglected.
- Current density is uniform in the conductor sections.
- Winding resistances are considered constant (do not vary with temperature).

II.11.1. Representation of the ASM in the electrical space

Figure II.17 shows the basic structure of the three-phase ASM. It includes the three stator windings and the three rotor windings, which the angle θ represents the position of the rotor phase (*ORa*) relative to that of the stator phase (*OSa*).

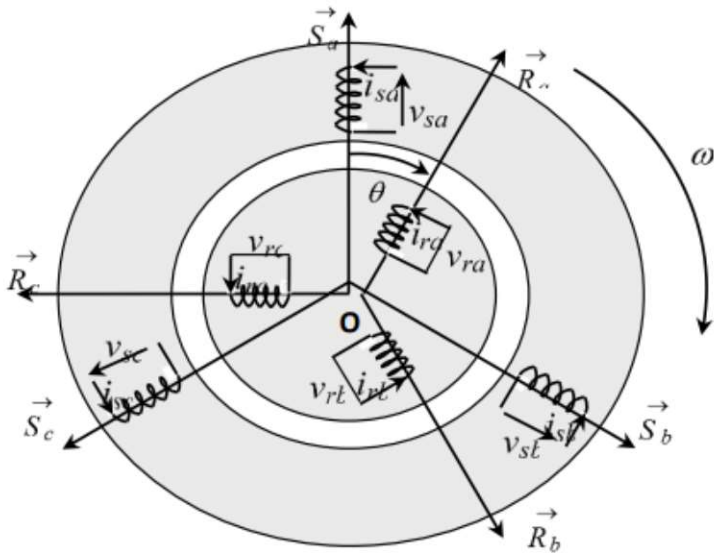

Figure II.9: Schematic representation of ASM

II.11.2. Mathematical model of ASM

The ASM model can be described by the following equations:

II.11.2.1. Electrical equations

The voltage equations of the stator and rotor phases are written in matrix form as follows:

$$[V_s] = R_s[I_s] + \frac{d}{dt}[\emptyset_s]$$
$$[V_r] = 0 = R_r[I_r] + \frac{d}{dt}[\emptyset_r] \quad \text{(II.27)}$$

Where:

$[V_S] = [V_{sa}, V_{sb}, V_{sc}]^t$ and $[V_r] = [V_{ra}, V_{rb}, V_{rc}]^t$: represent the voltages of the three stator and rotor phases, respectively.

$[I_S] = [I_{sa}, I_{sb}, I_{sc}]^t$ et $[I_r] = [I_{ra}, I_{rb}, I_{rc}]^t$: are the vectors of the currents flowing through these phases.

$[\phi_S] = [\phi_{sa}, \phi_{sb}, \phi_{sc}]^t$ et $[\phi_r] = [\phi_{ra}, \phi_{rb}, \phi_{rc}]$: correspond to the vectors of the total fluxes passing through the stator and rotor windings, respectively.

Rs and Rr : stator and rotor phase resistance, respectively.

The stator and rotor resistances matrices of the ASM are given by:

$$[R_s] = \begin{bmatrix} R_s & 0 & 0 \\ 0 & R_s & 0 \\ 0 & 0 & R_s \end{bmatrix} \qquad [R_r] = \begin{bmatrix} R_r & 0 & 0 \\ 0 & R_r & 0 \\ 0 & 0 & R_r \end{bmatrix} \tag{II.28}$$

II.11.2.2. Magnetic equations

The assumptions we have presented lead to linear relationships between flux and currents. They are expressed in matrix form as follows :

$$\begin{bmatrix} [\emptyset_s] \\ [\emptyset_r] \end{bmatrix} = \begin{bmatrix} [L_{ss}] & [M_{sr}] \\ [M_{rs}] & [L_{rr}] \end{bmatrix} \begin{bmatrix} [I_s] \\ [I_r] \end{bmatrix} \tag{II.29}$$

With :

$$[L_{ss}] = \begin{bmatrix} l_{ss} & M_{ss} & M_{ss} \\ M_{ss} & l_{ss} & M_{ss} \\ M_{ss} & M_{ss} & l_{ss} \end{bmatrix} \qquad [L_{rr}] = \begin{bmatrix} l_{rr} & M_{rr} & M_{rr} \\ M_{rr} & l_{rr} & M_{rr} \\ M_{rr} & M_{rr} & l_{rr} \end{bmatrix} \tag{II.30}$$

$$[M_{sr}] = m_{sr} \begin{bmatrix} \cos\theta & \cos\left(\theta + \frac{2\pi}{3}\right) & \cos\left(\theta - \frac{2\pi}{3}\right) \\ \cos\left(\theta - \frac{2\pi}{3}\right) & \cos\theta & \cos\left(\theta + \frac{2\pi}{3}\right) \\ \cos\left(\theta + \frac{2\pi}{3}\right) & \cos\left(\theta - \frac{2\pi}{3}\right) & \cos\theta \end{bmatrix} \tag{II.31}$$

l_{ss} and l_{rr} : Proper inductance of stator and rotor phase, respectively.

M_{ss} and M_{rr}: Mutual inductances between two stator phases and between two rotor phases, respectively.

m_{sr}: Maximum value of the mutual inductance between stator and rotor phase.

II.11.2.3. Mechanical equations

The fundamental relation of dynamics allows us to write:

$$C_{em} - C_l = J\frac{d\Omega}{dt} + f\Omega \tag{II.32}$$

With :

$$\Omega = \frac{\omega_r}{P} \tag{II.33}$$

Where:

C_{em}: represents the electromagnetic motor torque.

C_l: represents the load torque.

J: the moment of inertia of all rotating parts.

f: the friction coefficient.

To solve this issue, we are seeking methods to transform the three-phase variables of the ASM, which will enable us to go from the three-phase reference of the actual machine to either a fixed or rotating two-phase reference with respect to the stator or rotor.

II.12. Two-phases modeling of ASM

II.12.1. Park transformation

The two-phase model of the ASM is achieved by transforming the three-phase reference frame into a two-phase reference frame, which is essentially a change of basis on physical values (voltages, fluxes, and currents). This transformation leads to relationships independent of the angle θ and reduces the order of the machine equations. The Park transformation represents the direct axis d of the Park reference frame, and the quadrature axis q is shown in Figure II.10 [32], [33].

The figures II.10-11 illustrate the principle of the Park transformation applied to the ASM.

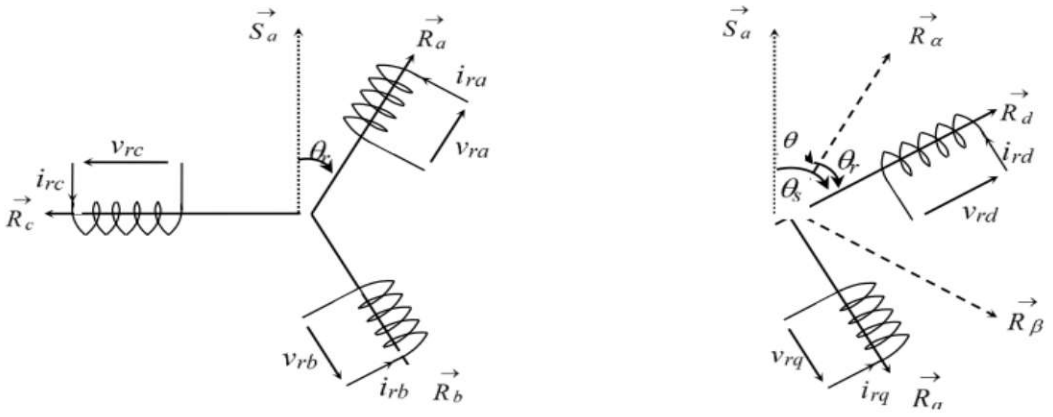

Figure II.10: Angular positioning of the (d,q) axis system associated with the stator of the ASM.

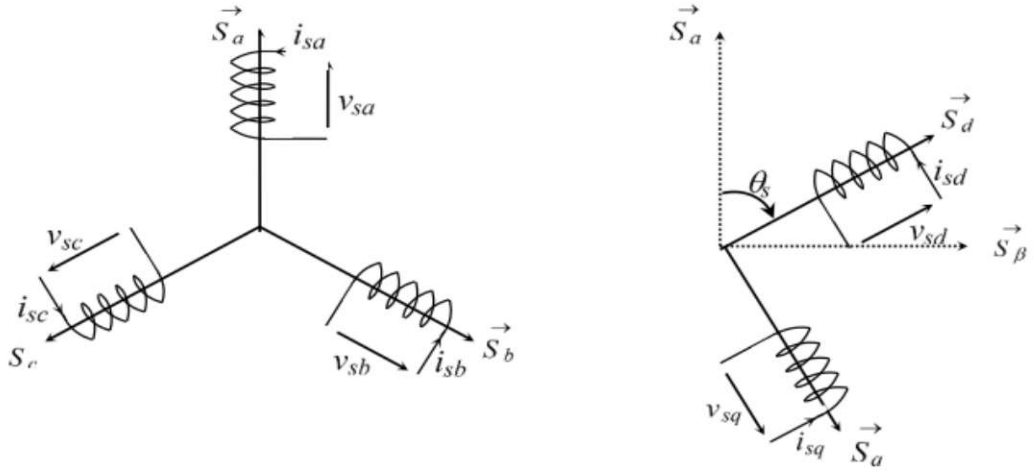

Figure II.11: Angular positioning of the (d,q) axis system associated with the rotor of the ASM.

To simplify the equations, the Park references of the stator and rotor values must coincide, which is possible through the following relationship:

$$\theta = \theta_s - \theta_r \tag{II.34}$$

So we define the Park transformation matrix as follows:

$$[P(\theta)] = \sqrt{\frac{2}{3}}\begin{bmatrix} \mathbf{Cos}\,\boldsymbol{\theta} & \mathbf{Cos}\left(\boldsymbol{\theta}-\frac{2\pi}{3}\right) & \mathbf{Cos}\left(\boldsymbol{\theta}-\frac{4\pi}{3}\right) \\ -\mathbf{Sin}\,\boldsymbol{\theta} & -\mathbf{Sin}\left(\boldsymbol{\theta}-\frac{2\pi}{3}\right) & -\mathbf{Sin}\left(\boldsymbol{\theta}-\frac{4\pi}{3}\right) \\ \frac{1}{\sqrt{2}} & \frac{1}{\sqrt{2}} & \frac{1}{\sqrt{2}} \end{bmatrix} \tag{II.35}$$

And the inverse transformation matrix by:

$$[P(\theta)]^{-1} = \sqrt{\frac{2}{3}}\begin{bmatrix} \mathbf{Cos}\,\boldsymbol{\theta} & -\mathbf{Sin}\,\boldsymbol{\theta} & \frac{1}{\sqrt{2}} \\ \mathbf{Cos}\left(\boldsymbol{\theta}-\frac{2\pi}{3}\right) & -\mathbf{Sin}\left(\boldsymbol{\theta}-\frac{2\pi}{3}\right) & \frac{1}{\sqrt{2}} \\ \mathbf{Cos}\left(\boldsymbol{\theta}-\frac{4\pi}{3}\right) & -\mathbf{Sin}\left(\boldsymbol{\theta}-\frac{4\pi}{3}\right) & \frac{1}{\sqrt{2}} \end{bmatrix} \tag{II.36}$$

This transformation generally allows the transition from the three-phase system a, b, c to two-phase system regardless of the electrical or electromagnetic values (flux, current, and voltage).

The change of variables related to currents, voltages, and fluxes is defined by:

$$\begin{bmatrix} X_d \\ X_q \\ X_o \end{bmatrix} = [P(\theta)] \begin{bmatrix} X_a \\ X_b \\ X_c \end{bmatrix} \quad \text{(II.37)}$$

With: X =V,I,ϕ

The inverse transformation is obtained by:

$$\begin{bmatrix} X_a \\ X_b \\ X_c \end{bmatrix} = [P(\theta)]^{-1} \begin{bmatrix} X_d \\ X_q \\ X_o \end{bmatrix} \quad \text{(II.38)}$$

For a balanced three-phase system, we have: $X_a+X_b+X_c=0$

This implies that the 'o' index component (homopolar component) is zero.

II.12.2. Electrical equations in the PARK reference frame

Stator and rotor equations:

$$\begin{cases} V_{sd} = R_s I_{sd} + \frac{d\emptyset_{sd}}{dt} - \frac{d\emptyset_s}{dt}\emptyset_{sq} \\ V_{sq} = R_s I_{sq} + \frac{d\emptyset_{sq}}{dt} - \frac{d\emptyset_s}{dt}\emptyset_{sd} \\ V_{rd} = 0 = R_r I_{rd} + \frac{d\emptyset_{rd}}{dt} - \frac{d\emptyset_r}{dt}\emptyset_{rq} \\ V_{rq} = 0 = R_r I_{rq} + \frac{d\emptyset_{rq}}{dt} - \frac{d\emptyset_r}{dt}\emptyset_{rd} \end{cases} \quad \text{(II.39)}$$

Applying the Park transformation to the flux and current equations (II-29), we obtained the electromagnetic relationships of the machine:

$$\begin{cases} \emptyset_{sd} = L_s i_{sd} + L_m i_{rd} \\ \emptyset_{sq} = L_s i_{sq} + L_m i_{rq} \\ \emptyset_{rd} = L_r i_{rd} + L_m i_{sd} \\ \emptyset_{rq} = L_r i_{rq} + L_m i_{sq} \end{cases} \quad \text{(II.40)}$$

II.13. Modeling of the flywheel

The part of the electromechanical system that allows storing kinetic energy is the flywheel. The amount of energy that can be stored in the flywheel is as follows:

$$Ec = \frac{1}{2} J\omega^2 \quad \text{(II.41)}$$

With:

J: represents the moment of inertia,

ω: represents the angular velocity.

We will only focus on the moment of inertia that is proportional to a fixed axis. The moment of inertia characterizes the geometry of the masses of a solid, it is a function of the mass and the shape of the rotating part:

$$J = \iiint x^2 + dm_x \quad \text{(II.42)}$$

With:

X: distance from the point to the centre of rotation,

dm_x : element of the associated mass.

Equation (II.42) can be simplified by [36]:

$$J = K\,M\,R^2 \quad \text{(II.43)}$$

With:

M: The rotating mass,

R: The maximum radius of the steering wheel,

K: A coefficient of form that takes different values according to the geometry of the steering

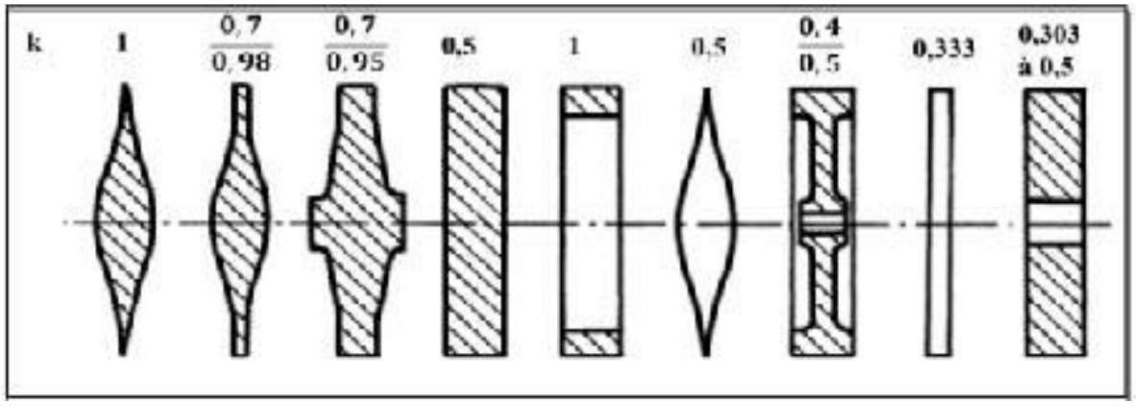

Figure II.12: Form factor k for different wheel geometries [37], [38].

wheel (see Figure II.12 and Table II.1).

Optimal shapes are obtained with a k value close to unity, but they are difficult to manufacture. Generally, a cylindrical shape is preferred. Regarding the solid perforated disk, $\boldsymbol{k}$ depends on the ratio of the inner and outer rays R_{int}/R_{ext}. For a large R_{ext}, $k \approx 0.3$, and for $R_{int} = R_{ext}$, we are in the case of a thin ring (k = 0.5)

Table II.1: Moments of inertia for different geometric shapes

The geometric shape of a mass M with radius R.	**Inertia moment J**
Iso disk under load	$\boldsymbol{J = MR^2}$
Thin ring	$\boldsymbol{J = \frac{1}{2}MR^2}$
Solid disk	$\boldsymbol{J = \frac{1}{2}MR^2}$
ball	$\boldsymbol{J = 0.4MR^2}$
sphere	$\boldsymbol{J = \frac{2}{3}MR^2}$

The total moment of inertia of the ELMS (electrical machine + flywheel) should not only consider that of the flywheel, but also that of the electrical machine.

To better understand, in Figure II.13, we have an example of the electromechanical part of ELMS. To calculate the inertia of this ELMS, we need to add the inertia of the motor, shaft, and flywheel rotor.

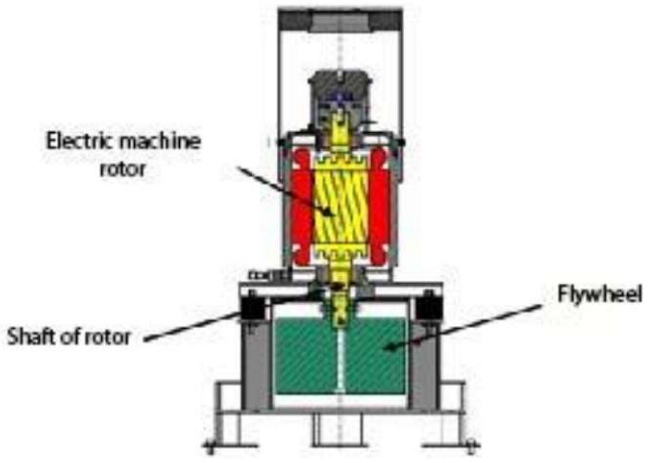

Figure II.13: Electromechanical part of ELMS [39].

The rotor and the shaft of the ASM is solid disks. The flywheel is perforated, but a long bolt is used for its axial attachment to the flywheel shaft, so it is considered a solid disk. Their inertia is therefore :

$$J = \frac{L}{2}\rho\pi r^4 \tag{II.44}$$

With:

ρ: The volumetric mass density, which is 7850 kg/m³ for the above-mentioned ELMS, is used to calculate the inertia of the components.

L: the height of the cylinder considered.

II.14. Modeling of synchronous generator

Rotating electrical machines are physical systems governed by electrical, magnetic, mechanical, thermal, and other phenomena. However, for the purposes of observing the position and speed of these machines, only electromagnetic and electromechanical phenomena are relevant for the implementation of a simplified and representative model [40].

II.14.1 Mathematical Model

Under the classical modeling assumptions for the control of electrical machines, we consider a synchronous machine with a wound rotor and *2p* salient poles. We apply the modeling principles to this machine.

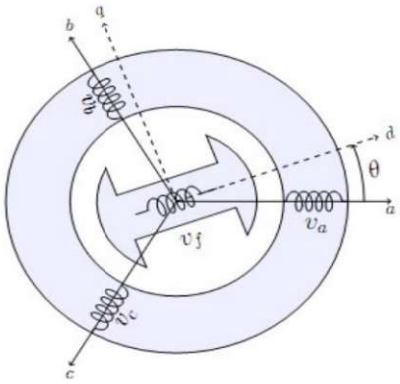

Figure II.14: The symbolic representation of a synchronous machine with a wound rotor and salient poles

II.14.2 Magnetic equations

According to Ampere's theorem, any current i flowing through a circuit generates a magnetic field across the area it encloses. The inductance of this circuit is the ratio of the magnetic flux ψ created by this field to the current flowing through the circuit.

Given an AC machine with n windings, the magnetic interactions between windings acting on a coil j involve:

- The self-inductances (θ).
- The mutual inductances (θ).

The inductances depend on the magnetic paths of the fluxes, so they are functions of the relative position of the rotor with respect to the stator. If ψj is the flux of the winding of circuit j, its expression in terms of the inductances and the currents ik flowing through circuits k is (the time dependence of the currents and fluxes is removed for simplicity) :

$$\begin{bmatrix} \Psi_1(t) \\ \Psi_2(t) \\ \vdots \\ \Psi_n(t) \end{bmatrix} = \begin{bmatrix} L_1(\theta) & M_{12}(\theta) & \cdots & M_{1n}(\theta) \\ M_{21}(\theta) & L_2(\theta) & \cdots & M_{2n}(\theta) \\ \vdots & \vdots & \ddots & \vdots \\ M_{n1}(\theta) & M_{n2}(\theta) & \cdots & L_n(\theta) \end{bmatrix} \begin{bmatrix} i_1(t) \\ i_2(t) \\ \vdots \\ i_n(t) \end{bmatrix} \quad \text{(II.45)}$$

Or in implicit form:

$$\Psi = \mathcal{L}(\theta)\, I \quad \text{(II.46)}$$

Under the assumption of sinusoidal distribution of the m.m.f, the inductance matrix is written as follows:

$$\mathcal{L}(\theta) = \mathcal{L}_0(\theta) + \mathcal{L}_2(\theta) \quad \text{(II.47)}$$

Where $\mathcal{L}_0$ is a constant matrix containing the position-independent inductances, and $\mathcal{L}_2(\theta)$ is a position-dependent matrix containing the inductances that vary with position; the subscript '2' indicates that only the second harmonic in the spatial distribution of inductances will be considered. The inductance matrix $\mathcal{L}(\theta)$ is symmetric due to the reciprocity of mutual inductances (Mij(θ) = Mji(θ)), thus :

$$\mathcal{L}(\theta) = \mathcal{L}^T(\theta) \quad \text{(II.48)}$$

The machine fluxes are expressed as follows:

$$\Psi_{3S} = \mathcal{L}_{3s}(\theta)\, I_{3s} + \mathcal{M}_{sf}(\theta)\, I_f \quad \text{(II.49)}$$

$$\Psi_f = \mathcal{M}_{sf}^{\mathrm{T}}(\theta)\, I_{3s} + \mathcal{L}_f(\theta)\, I_f \tag{II.50}$$

In the salient-pole synchronous reluctance motor, the inductance matrix $\mathcal{L}_{3s}(\theta)$ consists of two terms: a constant term $\mathcal{L}_{3s}$ and a term $\mathcal{L}_{3s2}(\theta)$ that varies with the electrical angle θ :

$$\mathcal{L}_{3s}(\theta) = \mathcal{L}_{3s0} + \mathcal{L}_{3s2}(\theta) \tag{II.51}$$

Where:

$$\mathcal{L}_{3s0} = \begin{bmatrix} L_{s0} & M_{s0} & M_{s0} \\ M_{s0} & L_{s0} & M_{s0} \\ M_{s0} & M_{s0} & L_{s0} \end{bmatrix} \tag{II.52}$$

And:

$$\mathcal{L}_{3s2}(\theta) = L_{s2} \begin{bmatrix} \cos(2\theta) & \cos\left(2\theta - \frac{2\pi}{3}\right) & \cos\left(2\theta + \frac{2\pi}{3}\right) \\ \cos\left(2\theta - \frac{2\pi}{3}\right) & \cos\left(2\theta + \frac{2\pi}{3}\right) & \cos(2\theta) \\ \cos\left(2\theta + \frac{2\pi}{3}\right) & \cos(2\theta) & \cos\left(2\theta - \frac{2\pi}{3}\right) \end{bmatrix} \tag{II.53}$$

Regarding $\mathcal{M}_{sf}(\theta)$, which is the mutual inductance between the rotor winding and the stator windings, it has the following expression:

$$\mathcal{M}_{sf}(\theta) = M_0 \begin{bmatrix} \cos(\theta) \\ \cos\left(\theta - \frac{2\pi}{3}\right) \\ \cos\left(2\theta + \frac{2\pi}{3}\right) \end{bmatrix} \tag{II.54}$$

II.14.3. Electromagnetic torque

The general expression of torque:

$$\begin{aligned} C_m &= \frac{p}{2} I^T \frac{\partial \mathcal{L}(\theta)}{\partial \theta} I \\ &= \frac{p}{2} \begin{bmatrix} I_{3s} \\ i_f \end{bmatrix}^T \frac{\partial}{\partial \theta} \left(\begin{bmatrix} \mathcal{L}_{3s}(\theta) & \mathcal{M}_{sf}(\theta) \\ \mathcal{M}_{sf}^T(\theta) & L_f \end{bmatrix} \right) \begin{bmatrix} I_{3s} \\ i_f \end{bmatrix} \end{aligned} \tag{II.55}$$

Taking equality into account :

$$I_{3s}^T \frac{d\mathcal{M}_{sf}}{d\theta} i_f = i_f \frac{d\mathcal{M}_{sf}^T}{d\theta} I_{3s} \tag{II.56}$$

W will have :

$$C_m = \frac{p}{2} I_{3s}^T \frac{d\mathcal{L}_{3s}}{d\theta} I_{3s} + P I_{3s}^T \frac{d\mathcal{M}_{sf}}{d\theta} i_f \quad \text{(II.57)}$$

- The first term, depending on the currents and stator inductances, describes the effect of saliency.
- The second term represents the torque generated by the interaction of stator and rotor fluxes. It exists for machines with excited rotor (by magnets or windings), where it is often the dominant term.

II.14.4. Modeling in the two-phase frame αβ

The fixed two-phase reference frame, linked to the stator, is noted αβ for the synchronous machine. The equations in this frame are derived from the projection of the three-phase equations by applying the Concordia transformation. This transformation is defined for all magnetic and electrical variables by the equation:

$$X_{\alpha\beta} = T_{32}^T X_{abc} = \sqrt{\frac{2}{3}} \begin{bmatrix} 1 & \frac{-1}{2} & \frac{-1}{2} \\ 0 & \frac{\sqrt{3}}{2} & \frac{-\sqrt{3}}{2} \end{bmatrix} \begin{bmatrix} X_a \\ X_b \\ X_c \end{bmatrix} \quad \text{(II.58)}$$

The diagram of the two-phase machine, equivalent in the sense of Concordia, is shown in Figure II.15, following the application of the three-phase to two-phase transformation.

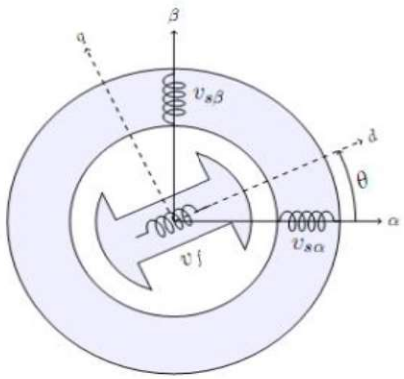

Figure II.15: Symbolic representation of the MSRB with prominent poles equivalent to the Concordia

II.14.5. Magnetic equations

The following factorizes inductance matrices in order to reveal the usual matrices of three-phase machines. Under the assumption of balanced three-phase system (the sum of stator currents is zero), we can express the constant part of the inductance matrix, which is a symmetric circulant matrix, in the following form:

$$\mathcal{L}_{3s0} = (L_{s0} M_{s0}) T_{32} T_{32}^{T} \tag{II.59}$$

The variable (position-dependent) part of the inductance matrix, $\mathcal{L}_{3s2}(\theta)$, which is symmetric but not circulant, can be expressed in the following manner:

$$\mathcal{L}_{3s2}(\theta) = \frac{3}{2} L_{s2} T_{32} P(\theta) K_2 P(-\theta) T_{32}^{T} \tag{II.60}$$

The matrix K_2 is a 2×2 matrix analogous to the complex conjugation operation for complex numbers, and it is written as:

$$K_2 = \begin{bmatrix} 1 & 0 \\ 0 & -1 \end{bmatrix} \tag{II.61}$$

Finally, the stator inductance matrix is written in the following factored form:

$$\mathcal{L}_{3s} = \mathcal{L}_{3s0} + \mathcal{L}_{3s2} = T_{32}[L_0 I_2 + L_2 P(\theta) K_2 P(-\theta)] T_{32}^{T} \tag{II.62}$$

With :

$$L_0 = L_{s0} - M_{s0} \tag{II.63}$$

$$L_2 = \frac{3}{2} L_{s2} \tag{II.64}$$

Regarding $\mathcal{M}_{sf}(\theta)$, it can be factored as follows:

$$\mathcal{M}_{sf}(\theta) = \sqrt{\frac{3}{2}}\, M_0 T_{32} P(\theta) \begin{bmatrix} 1 \\ 0 \end{bmatrix} = M_f T_{32} \begin{bmatrix} \cos(\theta) \\ \sin(\theta) \end{bmatrix} \tag{II.65}$$

Where : $M_f = \sqrt{\frac{3}{2}}\, M_0$ (II.66)

- **Stator flux**

Let's apply the Concordia transformation to the stator flows:

$$\Psi_f = T_{32} \Psi_{s\alpha\beta} = \mathcal{L}_{s\alpha\beta}(\theta) T_{32} I_{s\alpha\beta} + \mathcal{M}_{sf}(\theta) i_f \tag{II.67}$$

Multiplying left by T_{32}^{T}, we obtain :

$$\Psi_{s\alpha\beta} = \mathcal{L}_{s\alpha\beta}\, I_{s\alpha\beta} + M_f I_{f\alpha\beta} \tag{II.68}$$

Where $\mathcal{L}_{s\alpha\beta}$ is the stator inductance matrix in the $\alpha\beta$ two-phase coordinate system:

$$\begin{aligned}\mathcal{L}_{s\alpha\beta} &= L_0 I_2 + L_2 P(\theta) K_2 P(-\theta) \\ &= \begin{bmatrix} L_0 + L_2\cos(2\theta) & L_2\sin(2\theta) \\ L_2\sin(2\theta) & L_0 - L_2\cos(2\theta) \end{bmatrix}\end{aligned} \tag{II.69}$$

And $I_{f\alpha\beta}$ is the vector of projections of the rotor current in the $\alpha\beta$ coordinate system:

$$I_{f\alpha\beta} = i_f[\cos(\theta) \quad \sin(\theta)]^T \tag{II.70}$$

- **Rotor flux**

The rotor flux in the fixed two-phase reference frame is expressed as follows:

$$\begin{aligned}\Psi_{f\alpha\beta} &= \Psi_f \begin{bmatrix}\cos(\theta)\\ \sin(\theta)\end{bmatrix} \\ &= M_{sf}^T I_{3s} \begin{bmatrix}\cos(\theta)\\ \sin(\theta)\end{bmatrix} + L_f I_{f\alpha\beta} \\ &= M_{f\alpha\beta} I_{s\alpha\beta} + L_f I_{f\alpha\beta}\end{aligned} \tag{II.71}$$

With:

$$\begin{aligned}M_{f\alpha\beta}(\theta) &= M_f \begin{bmatrix} \cos^2(\theta) & \cos(\theta)\sin(\theta) \\ \cos(\theta)\sin(\theta) & \sin^2(\theta) \end{bmatrix} \\ &= \frac{M_f}{2}\begin{bmatrix} 1+\cos(2\theta) & \sin(2\theta) \\ \sin(2\theta) & 1-\cos(2\theta) \end{bmatrix}\end{aligned} \tag{II.72}$$

Finally, the flow equations are written:

$$\Psi_{s\alpha} = (L_0 + L_2\cos(2\theta))i_{s\alpha} + L_2 i_{s\beta}\sin(2\theta) + M_f i_{f\alpha} \tag{II.73}$$

$$\Psi_{s\beta} = (L_0 - L_2\cos(2\theta))i_{s\beta} + L_2 i_{s\alpha}\sin(2\theta) + M_f i_{f\beta} \tag{II.74}$$

$$\Psi_{f\alpha} = L_f i_{f\alpha} + M_f i_{s\alpha}\cos^2(\theta) + M_f i_{s\beta}\cos(\theta)\sin(\theta) \tag{II.75}$$

$$\Psi_{f\beta} = L_f i_{f\beta} + M_f i_{s\beta}\sin^2(\theta) + M_f i_{s\alpha}\cos(\theta)\sin(\theta) \tag{II.76}$$

Or in matrix form :

(II.77)

$$\begin{bmatrix}\Psi_{s\alpha\beta}\\ \Psi_{f\alpha\beta}\end{bmatrix} = \mathcal{L}(\theta)I = \begin{bmatrix}\mathcal{L}_{s\alpha\beta} & M_f I_2\\ \mathcal{M}_{f\alpha\beta} & L_f I_2\end{bmatrix}\begin{bmatrix}I_{s\alpha\beta}\\ I_{f\alpha\beta}\end{bmatrix}$$

II.14.6. Electrical equations

Let's apply the Concordia transformation for equations ($\vartheta_{3s} = R_s I_{3s} + \frac{d\Psi_{3s}}{dt}$) and ($\upsilon_f = R_f i_f + \frac{d\Psi_f}{dt}$) taking into account of equation (II.76), at the stator we obtain:

$$\vartheta_{s\alpha\beta} = R_s I_{s\alpha\beta} + \frac{d\Psi_{s\alpha\beta}}{dt} \tag{II.78}$$

$$= R_s I_{s\alpha\beta} + \mathcal{L}_{s\alpha\beta}\frac{dI_{s\alpha\beta}}{dt} + M_f\frac{dI_{f\alpha\beta}}{dt} + \omega\frac{d\mathcal{L}_{s\alpha\beta}}{d\theta}I_{s\alpha\beta}$$

With:

$$\frac{dI_{f\alpha\beta}}{dt} = \begin{bmatrix}-\sin(\theta)\\ \cos(\theta)\end{bmatrix} i_f\omega + \begin{bmatrix}\cos(\theta)\\ \sin(\theta)\end{bmatrix}\frac{di_f}{dt} \tag{II.79}$$

$$\frac{d\mathcal{L}_{s\alpha\beta}}{d\theta} = \begin{bmatrix}-2L_2\sin(2\theta) & 2L_2\cos(2\theta)\\ 2L_2\cos(2\theta) & 2L_2\sin(2\theta)\end{bmatrix} \tag{II.80}$$

Or in the explicit matrix form:

$$\begin{bmatrix}\upsilon_{s\alpha}\\ \upsilon_{s\beta}\end{bmatrix} = R_s\begin{bmatrix}i_{s\alpha}\\ i_{s\beta}\end{bmatrix} + \begin{bmatrix}L_0 + L_2\cos(2\theta) & L_2\sin(2\theta)\\ L_2\sin(2\theta) & L_0 - L_2\cos(2\theta)\end{bmatrix}\begin{bmatrix}\frac{di_{s\alpha}}{dt}\\ \frac{di_{s\beta}}{dt}\end{bmatrix}$$
$$+ M_f\left(\begin{bmatrix}-\sin(\theta)\\ \cos(\theta)\end{bmatrix} i_f\omega + \begin{bmatrix}\cos(\theta)\\ \sin(\theta)\end{bmatrix}\frac{di_f}{dt}\right) \tag{II.81}$$
$$+ \omega\begin{bmatrix}-2L_2\sin(2\theta) & 2L_2\cos(2\theta)\\ 2L_2\cos(2\theta) & 2L_2\sin(2\theta)\end{bmatrix}\begin{bmatrix}i_{s\alpha}\\ i_{s\beta}\end{bmatrix}$$

While at the rotor we get:

$$\vartheta_{f\alpha\beta} = R_f I_{f\alpha\beta} + \frac{d\Psi_{f\alpha\beta}}{dt}$$

$$= R_f I_{f\alpha\beta} + \frac{dI_{s\alpha\beta}}{dt} + L_f\frac{dI_{f\alpha\beta}}{dt} + \omega\frac{d\mathcal{M}_{f\alpha\beta}}{d\theta}I_{s\alpha\beta} \tag{II.82}$$

With:

$$\frac{d\mathcal{M}_{f\alpha\beta}}{d\theta} = M_f\begin{bmatrix}-\sin(2\theta) & \cos(2\theta)\\ \cos(2\theta) & \sin(2\theta)\end{bmatrix} \tag{II.83}$$

Or in the explicit matrix form:

$$\begin{bmatrix} v_{f\alpha} \\ v_{f\beta} \end{bmatrix} = R_f i_f \begin{bmatrix} \cos(\theta) \\ \sin(\theta) \end{bmatrix} + \frac{M_f}{2} \begin{bmatrix} 1+\cos(2\theta) & \sin(2\theta) \\ \sin(2\theta) & 1-\cos(2\theta) \end{bmatrix} \begin{bmatrix} \frac{di_{s\alpha}}{dt} \\ \frac{di_{s\beta}}{dt} \end{bmatrix}$$
$$+ L_f \left(\begin{bmatrix} -\sin(\theta) \\ \cos(\theta) \end{bmatrix} i_f \omega + \begin{bmatrix} \cos(\theta) \\ \sin(\theta) \end{bmatrix} \frac{di_f}{dt} \right) + \omega M_f \begin{bmatrix} -\sin(2\theta) & \cos(2\theta) \\ \cos(2\theta) & \sin(2\theta) \end{bmatrix} \begin{bmatrix} i_{s\alpha} \\ i_{s\beta} \end{bmatrix} \quad \text{(II.84)}$$

II.14.7. Electromagnetic torque

Let's apply the Concordia transformation to equation (II.57), and then the expression of the torque is written as follows:

$$C_m = \frac{P}{2} I^T \frac{\partial \mathcal{L}(\theta)}{\partial \theta} I = \frac{P}{2} I_{s\alpha\beta}^T + \frac{P}{2} I_{f\alpha\beta}^T \frac{\partial \mathcal{M}_{f\alpha\beta}}{\partial \theta} I_{s\alpha\beta} \quad \text{(II.85)}$$
$$= PM_f i_f \left(i_{s\beta} \cos(\theta) - i_{s\alpha} \sin(\theta) \right) - PL_2 \left[\left(i_{s\alpha}^2 - i_{s\beta}^2 \right) \sin(2\theta) - 2 i_{s\alpha} i_{s\beta} \cos(2\theta) \right]$$

II.14.8. Modeling in the rotating dq reference frame

$$\mathrm{X}_{\alpha\beta} = \mathrm{P}(\theta)\mathrm{X}_{\mathrm{dq}} \quad \text{(II.86)}$$

The equivalent two-phase machine diagram, in the Park sense, is presented in Figure II.16, after the application of the Park transformation.

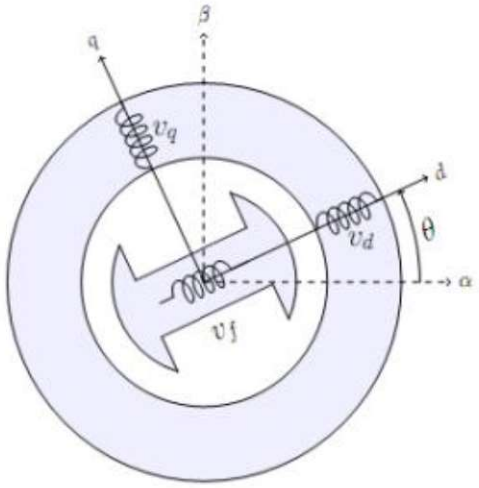

Figure II.16: Symbolic representation of the MSRB with prominent poles equivalent to the Park sense.

II.14.9. Magnetic equations

The stator inductance matrix (II.73) in the fixed two-phase reference frame factorizes as follows:

$$\begin{aligned}\mathcal{L}_{s\alpha\beta} &= P(\theta)(L_0 I_2 + L_2 K_2)P(-\theta) \\ &= P(\theta)\mathcal{L}_{sdq}P(-\theta)\end{aligned} \tag{II.87}$$

Where :

$$\mathcal{L}_{s\alpha\beta} = \begin{bmatrix} L_d & 0 \\ 0 & L_q \end{bmatrix} \tag{II.88}$$

With L_d and L_q being the direct-axis (d) and quadrature-axis (q) inductances respectively:

$$L_d = L_0 + L_2 \tag{II.89}$$

$$L_q = L_0 - L_2 \tag{II.90}$$

The mutual inductance between the stator windings and the rotor winding factorizes as follows:

$$\mathcal{M}_{sf} = M_f T_{32} P(\theta) \begin{bmatrix} 1 \\ 0 \end{bmatrix} \tag{II.91}$$

The zero component in the right-hand vector of equation (II.91) arises from the fact that only the direct axis of the rotor is excited by the current i*f*.

- **Stator flux**

  From the factored forms of the inductance matrices, applying the rotation transformation to the stator fluxes, by left-multiplying equation (II.68) by P(−θ):

$$\Psi_{sdq} = \mathcal{L}_{sdq} I_{sdq} + M_f I_{fdq} \tag{II.92}$$

The quadrature component of the rotor current vector in the dq frame is zero ($i_{fq} = 0$), while the direct-axis component is equal to the excitation current $i_{fd} = i_f$."

- **Rotor flux**

The components of the rotor flux vector $\Psi_{f\alpha\beta}$ are written as follows:

$$\Psi_{f\alpha} = M_f i_{sd} \cos(\theta) + L_f i_f \cos(\theta) \tag{II.93}$$

$$\Psi_{f\beta} = M_f i_{sd} \sin(\theta) + L_f i_f \sin(\theta) \tag{II.94}$$

Then, the components of the rotor flow in the dq frame are:

$$\Psi_{fd} = M_f i_{sd} + L_f i_f \quad \text{(II.95)}$$

$$\Psi_{fq} = 0 \quad \text{(II.96)}$$

According to equations (II.95) and (II.96), we can conclude that the d-axis is aligned with the rotor flux, which leads us to consider only the d-axis component when referring to the rotor flux. This allows us to simplify the notation by omitting the q index.

The MSRB flows in the dq frame are therefore written as:

$$\begin{bmatrix} \Psi_{sd} \\ \Psi_{sq} \\ \Psi_f \end{bmatrix} = \begin{bmatrix} L_d & 0 & M_f \\ 0 & L_q & 0 \\ M_f & 0 & L_f \end{bmatrix} \begin{bmatrix} i_{sd} \\ i_{sq} \\ i_f \end{bmatrix} \quad \text{(II.97)}$$

II.14.10. Electrical equations

Let's replace the variables Xsαβ with P(θ)Xsdq in equation (II.77), and left-multiply by the matrix P(−θ), using the properties of this matrix, we obtain:

$$\begin{aligned} \vartheta_{s\alpha\beta} &= R_s I_{sdq} + P(-\theta)\frac{d}{dt}\left(P(\theta)\Psi_{sdq}\right) \\ &= R_s I_{sdq} + \frac{d\Psi_{sdq}}{dt} + \omega P(-\theta) P\left(\theta + \frac{\pi}{2}\right)\Psi_{sdq} \\ &= R_s I_{sdq} + \frac{d\Psi_{sdq}}{dt} + \omega J_2 \Psi_{sdq} \end{aligned} \quad \text{(II.98)}$$

Proceeding in the same way for the rotor voltage (II.81), we obtain:

$$\vartheta_f = R_f I_f + \frac{d\Psi_f}{dt} \quad \text{(II.99)}$$

Finally, the MSRB voltage equations in the dq frame are written:

$$v_{sd} = R_s i_{sd} + L_d \frac{di_{sd}}{dt} + M_f \frac{di_f}{dt} - \omega L_q i_{sd} \quad \text{(II.100)}$$

$$v_{sq} = R_s i_{sq} + L_q \frac{di_{sq}}{dt} + \omega\left(M_f i_f + L_d i_{sd}\right) \quad \text{(II.101)}$$

$$v_f = R_f i_f + M_f \frac{di_{sd}}{dt} + L_f \frac{di_f}{dt} \quad \text{(II.102)}$$

II.14.11. Electromagnetic torque

Knowing that the electrical power transformed into mechanical power inside the motor is expressed as follows:

$$P_u = C_m \Omega \tag{II.103}$$

Where: Ω is the rotation speed.

And on the other hand, we have:

$$P_u = P\left(\Psi_{sd} i_{sq} - \Psi_{sq} i_{sd}\right)\Omega \tag{II.104}$$

According to equations (II.103) and (II.104), the couple equation is written as:

$$\begin{aligned} C_m &= P\left(\Psi_{sd} i_{sq} - \Psi_{sq} i_{sd}\right) \\ &= P\left[\left(L_d - L_q\right) i_{sd} + \mathrm{M}_f i_f\right] i_{sq} \end{aligned} \tag{II.105}$$

The matrix form is as follows:

$$C_m = P I_{sdq}^T J_2 \Psi_{sdq} \tag{II.106}$$

II.15. Conclusion

In this chapter, we have studied the static converters used in photovoltaic systems, such as the boost converter and the inverter, as well as the asynchronous motor. We presented the modeling of a single-diode PV cell, the heart of the PV generator, and the boost converter controlled by an MPPT algorithm. For this purpose, we chose the P&O method. The inverter control was performed using the SPWM technic. In the final phase of the chapter, we introduced a model of the asynchronous machine using PARK's transformation to simplify the equations by transitioning from a three-phase reference frame to a two-phase reference frame. Modeling each element of the photovoltaic system will allow us to simulate the PV system, analyze, and interpret the results obtained, modelling which allowed us to obtain two models one following the stator (αβ), and the other following the dq of the synchronous machine. Their simulations are the subject of the following chapter.

Chapter III
Control of the PV-Electromechanical system association

III.1. Introduction

In this chapter, we study the control of an asynchronous motor. In formulating any control problem, there are typically discrepancies between the real system and the mathematical model developed for control design.

We will focus on applying the sliding mode control technique to the asynchronous machine and establish the control value expressions based on the model established in the second chapter. We will also observe the various results obtained through simulation to enable an evaluation of the robustness and performance of this variable structure control mode.

This chapter also concerns our simulation of the electromechanical system coupled with the PV system by means of a DC/DC converter controlled by the P&O method in order to reach the maximum point of power regardless of the sunshine and temperature. An inverter based on a transistor controlled by PWM, asynchronous machine and synchronous generator.

The objective of this chapter is to achieve the electrical energy in the output of generator which is the last element linked to the system, also to see the important role of flywheel and the performance of global system under standard conditions of irradiation and temperature, and during the variation of ASM speed.

III.2. Principle of sliding mode control

Being a particular case of Variable Structure Control (V_{SC}), sliding mode control has been widely used in the literature. This success is due to its simplicity of implementation and its robustness against parametric variations and external disturbances. It involves first defining a sliding surface representing the desired dynamics, then synthesizing a control law that must act on the system in two phases. In the first phase, the system is forced to reach this surface, and in the second phase, it must ensure the maintenance and sliding along this surface to reach the origin of the phase plane [41].

III.3. Choice of sliding surface

The design of the control system will be demonstrated for the following nonlinear system:

$$\dot{x} = f(x,t) + g(x,t).u \qquad \text{(III.1)}$$

Where: $x \in \Re^*$ and the state vector $u \in \Re^m$ and the control vector, $f(x,t) \in \Re^n$, $g(x,t) \in \Re^{n*m}$

The general equation form for sliding surface, proposed by 'J.J.Slotinie' and ensuring the convergence of a variable to its desired value, is given by:

$$S(x) = \left(\frac{d}{dt} + \lambda\right)^{n-1} e \qquad \text{(III.2)}$$

With:

λ: Positive coefficient.

e: $x - x_d$

x_d: Desired value.

n: Order of the system is the smallest positive integer representing the number of times it must be differentiated for the control input to appear.

S(x): is an autonomous linear differential equation whose response "e" tends to zero for a correct choice of the gain λ , and this is the objective of the control.

The objective of this control is to keep the surface tending to zero. The latter is a linear differential equation whose unique solution is e(x) = 0 for a suitable choice of the parameterλ. This amounts to a trajectory-tracking problem, which is equivalent to an exact linearization of the error, while respecting the convergence condition [42].

- **Direct switching function**

The direct switching function is the first and oldest convergence condition, proposed and studied by EMILYANOV and UTKIN. It involves giving the surface a convergent dynamic towards zero. It is expressed in the form:

$$S(x).\dot{S(x)} < 0 \qquad \text{(III.3)}$$

- **Lyapunov Function**

The Lyapunov function is a positive scalar function V(x) > 0 for the system's state variables. The control law must cause this function V(x) < 0 to decrease. The idea is to choose a scalar function S(x) to ensure the attraction of the controlled variable towards its reference

value and to construct a control U such that the square of the sliding surface corresponds to a Lyapunov function. By defining the Lyapunov function as follows:

$$V(X) = \frac{1}{2}S^2(X) \tag{III.4}$$

By deriving (III.4), we obtain:

$$\dot{V}(X) = S(x).\dot{S(x)} \tag{III.5}$$

For the function V(x) to decrease, it is sufficient to ensure that its derivative is negative, $S(x).\dot{S(x)} < 0$. This is only satisfied if condition (III.5) is verified. Equation (III.4) explains that the square of the distance between a given point in the phase plane and the sliding surface, expressed by $S^2(x)$, decreases all the time, forcing the system trajectory to move towards the surface from both sides. This condition assumes an ideal sliding regime where the switching frequency is infinite [43]. This function is used to estimate the performance of the control, such as the robustness and stability of nonlinear systems.

III.4. Definition of control quantities

The structure of a sliding mode controller consists of two parts, one concerning the exact linearization $\mathbf{u_{eq}}$ and the other concerning stability $\mathbf{u_n}$. This last is very important in the sliding mode control technique because it is used to eliminate the effects of model imprecision and to reject external disturbances. Thus, the total control is given by [43]:

$$u = u_{eq} + u_n \tag{III.6}$$

u_{eq}: corresponds to the equivalent control proposed by Filippov and Utkin, and can be considered as the continuous average

III.5. Analytical expression of the order

We are interested in calculating the equivalent control and subsequently in calculating the attractive control of the system defined in the state space by equation (III.1).The vector u is composed of two quantities: $u_{eq} et\ u_n$, we have:

$$\dot{S} = \frac{ds}{dt} = \frac{\partial s}{\partial x}\frac{\partial x}{\partial t} = \frac{\partial s}{\partial x}\{f(x,t) + g(x,t).u_{eq}\} + \frac{\partial s}{\partial x}\{g(x,t).u_n\} \tag{III.7}$$

In sliding mode and under steady-state conditions, the derivative of the sliding surface is zero (since the surface equals zero). Thus, we obtain :

$$u_{eq} = -\left\{\frac{\partial s}{\partial x} g(x,t)\right\}^{-1} \left\{\frac{\partial s}{\partial x} f(x,t)\right\} \; u_n = 0 \qquad \text{(III.8)}$$

During the convergence mode, by replacing the term with its value (III.8) in equation (III.7), we obtain a new expression for the derivative of the sliding surface, which is:

$$\dot{S} = \frac{\partial s}{\partial x}\{g(x,t).u_n\} \qquad \text{(III.9)}$$

The problem becomes to finding u_n such that:

$$S(x).\dot{S}(x) = S(x)\frac{\partial s}{\partial x}\{g(x,t).u_n\} < 0 \qquad \text{(III.10)}$$

The simplest solution is to choose it in the form of a relay as shown in Figure (III.1). In this case, the control is written as follows [44]:

$$u_n = -K.sing(S) \qquad \text{(III.11)}$$

$$sing(S) = \begin{cases} 1 & si\ S > 0 \\ 0 & si\ S = 0 \\ -1 & si\ S < 0 \end{cases}$$

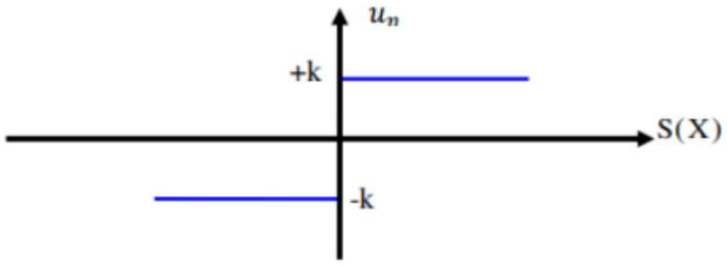

FigureIII.1: ''Sign'' function representation

By substituting expression (III.10) into (III.11), we obtain:

$$S(x).\dot{S(x)} = S(x)\frac{\partial s}{\partial x} g(x,t)K|S(x)| < 0 \qquad \text{(III.12)}$$

Where: the factor $S(x)\frac{\partial s}{\partial x} g(x,t)$ is always negative for the class of the system we have considered.

III.6. Sliding mode control

III.6.1. Synthesis of sliding mode control

The objective of this synthesis is to determine a control law to force the system states (speed and rotor flux), which are assumed and measured, to follow the sliding surface. The control system generates two stator voltage commands corresponding to the speed and rotor flux control. The asynchronous motor can be described by a fifth-order nonlinear system, with four electrical variables (stator currents, rotor fluxes), one mechanical variable (rotational speed), and two control variables (stator voltages).

The dynamic model of the asynchronous machine can be expressed in the form:

$$\begin{aligned}
\dot{x_1} &= f_1(x_1) + bu_1 \quad , \quad f_1 = -a_1x_1 + a_2x_3 + a_3x_5x_4 \\
\dot{x_2} &= f_2(x_2) + bu_2 \quad , \quad f_1 = -a_1x_2 + a_2x_4 - a_3x_4x_5 \\
\dot{x_3} &= f_3 \quad , \quad f_1 = a_4x_1 - a_5x_3 - a_6x_4x_5 \\
\dot{x_4} &= f_4 \quad , \quad f_1 = a_4x_2 - a_5x_4 + a_6x_3x_5 \\
\dot{x_5} &= f_5 \quad , \quad f_1 = a_7(a_3x_2 - a_1x_4) - a_8x_5 - a_9
\end{aligned} \tag{III.13}$$

III.7. Adjustment of the MAS speed by sliding mode control

III.7.1 Orientation of the rotor flux

Asynchronous motors face difficulties in control due to the complex coupling between various parameters such as magnetic flux, torque, speed, or position.
To solve this problem using rotor flux orientation, a type of vector control, this control technique is considered a powerful tool that can provide the same performance as separately excited DC motors. In this type of orientation, we have: $\phi = \phi_{rd} = \phi_r$, $\phi_{rq} = 0$.

The torque equation is given by:

$$C_e = \frac{1m}{L_r}\left(\phi_{rd}\, I_{sq} - \phi_{rq}\, I_{sd}\right) \tag{III.14}$$

When applying rotor flux orientation, the torque equation becomes:

$$C_e = \frac{PM}{L_r}\,\phi_{rd}\, I_{sq} \tag{III.15}$$

III.7.2 Explanation of the adjustment

The speed regulation is a cascade structure, where the inner loop controls the Isq current, with faster dynamics, while the outer loop controls the speed. To limit any stator current (torque) overshoot that could damage the system, select the saturation function.

The expression of the surface has the following form:

$$S(\Omega) = \Omega_{ref} - \Omega \tag{III.16}$$

The derivative is :

$$\dot{S}(\Omega) = \dot{\Omega}_{ref} - \dot{\Omega} \tag{III.17}$$

With :

$$\frac{d\Omega}{dt} = \frac{1}{J}\frac{\mathrm{PM}}{\mathrm{L}_r}\left(\phi_{rd}\,\mathrm{I}_{sq}\right) - \frac{1}{J}C_r - \frac{1}{J}f\Omega \tag{III.18}$$

Replacing the mechanical equation in the commutation surface equation:

$$\dot{S}(\Omega) = \Omega_{ref}^{\dot{e}} - \frac{1}{J}\frac{\mathrm{PM}}{\mathrm{L}_r}\left(\phi_{rd}\,\mathrm{I}_{sq}\right) - \frac{1}{J}C_r - \frac{1}{J}f\Omega \tag{III.19}$$

Reconciling the Isq current with the current $\mathrm{I}_{sq} = I_{sq}^{eq} + I_{sq}^{d}$, we find:

$$\dot{S}(\Omega) = \dot{\Omega}_{ref} - \left(\frac{1}{J}\frac{\mathrm{PM}}{\mathrm{L}_r}\,\phi_{rd}\,I_{sq}^{eq} + \frac{1}{J}\frac{\mathrm{PM}}{\mathrm{L}_r}\,\phi_{rd}\,I_{sq}^{d} - \frac{1}{J}C_r - \frac{1}{J}f\Omega\right) \tag{III.20}$$

When the sliding mode is in steady state, we have:

$$S(\Omega) = 0\,,\dot{S}(\Omega) = 0\,,I_{sq}^{d} = 0 \tag{III.21}$$

We extract from the previous equation the equivalent control quantity:

$$I_{sq}^{eq} = \left(\dot{\Omega}_{ref} + \frac{1}{J}C_r + \frac{1}{J}f\Omega\right)\frac{JL_r}{PM}\frac{1}{\phi_{rd}} \tag{III.22}$$

We substitute (III-21) into (III-22):

$$\dot{S}(\Omega) = -\frac{1}{J}\frac{PM}{L_r}\phi_{rd}I_{sq}^{d} \tag{III.23}$$

In the condition $\dot{V}(x) = S(x).\dot{S(x)} < 0$ during the convergence mode, must be verified, we pose:

$$I_{sq}^{d} = K_{I_{sq}} \cdot signe\big(S(\Omega)\big) \tag{III.24}$$

To verify the stability condition of the system, the parameter K_{Isq} must be positive. To mitigate any potential overshoot of the reference current, it is generally useful to add a current limiter, which is expressed as follows:

$$I_{sq}^{lim} = I_{sq}^{max} signe\big(S(\Omega)\big) \tag{III.25}$$

To reconcile the value of I_{sq}^{d}, we obtain:

$$\dot{S}(\Omega) = -\frac{1}{J}\frac{PM}{L_r}\phi_{rd} I_{sq}^{d} = \frac{1}{J}\frac{PM}{L_r}\phi_{rd} K_{I_{sq}} \cdot signe\big(S(\Omega)\big) \tag{III.26}$$

III.8. Set ASM current (I_{sd} and I_{sq}) by sliding mode

In this application, we will adjust the I_{sd} and I_{sq} currents by controlling the V_{sd} and V_{sq} voltages successively.

III.8.1. Setting of current I_{sd}

The expression of the surface takes the form:

$$S(I_{sd}) = I_{sd}^{ref} - I_{sd} \tag{III.27}$$

The derivative of the surface is:

$$\dot{S}(I_{sd}) = \dot{I_{sd}^{ref}} - \dot{I_{sd}} \tag{III.28}$$

From torque equation:

$$C_e = \frac{\mathrm{pm}}{\mathrm{L}_r}\left(\phi_{rd}\,\mathrm{I}_{sq} - \phi_{rq}\,\mathrm{I}_{sd}\right) \tag{III.29}$$

We have :

$$\frac{dI_{sd}}{dt} = -\frac{1}{\delta L_s}\left(R_s + \frac{R_r M^2}{L_r^2}\right) I_{sd} + \omega_s I_{sq} + \frac{1}{\delta L_s}\frac{R_r M}{L_r^2}\phi_{rd} + \frac{1}{\delta L_s}\frac{M}{L_r}\omega_r \phi_{rq} + \frac{1}{\delta L_s} V_{sd} \tag{III.30}$$

By replacing equation III.29 in the Lyapunov equation, the derivative of the surface becomes:

$$\dot{S}(I_{sd}) = \dot{I_{sd}^{ref}} - \left(-\frac{1}{\delta L_s}\cdot\left(R_s + \frac{R_r M^2}{L_r^2}\right) I_{sd} + \omega_s I_{sq} + \frac{1}{\delta L_s}\frac{R_r M}{L_r^2}\phi_{rd} + \frac{1}{\delta L_s}\frac{M}{L_r}\omega_r \cdot \right. \quad \text{(III.31)}$$

$$\left. \phi_{rq} + \frac{1}{\delta L_s} V_{sd}\right)$$

By replacing the voltage V_{sd} with $V_{sd} = V_{sq}^{eq} + V_{sq}^{d}$, the equation will be written in the following form:

$$\dot{S}(I_{sd}) = \dot{I_{sd}^{ref}} - \left(-\frac{1}{\delta L_s}\left(R_s + \frac{R_r M^2}{L_r^2}\right) I_{sd} + \omega_s I_{sq} + \frac{1}{\delta L_s}\frac{R_r M}{L_r^2}\phi_{rd} + \frac{1}{\delta L_s}\frac{M}{L_r}\omega_r\phi_{rq} + \frac{1}{\delta L_s}\right. \quad \text{(III.32)}$$

During the sliding mode and in steady state, we have:

$$S(I_{sd}), \dot{S}(I_{sd}),\ V_{sd}^{d} = 0 \quad \text{(III.33)}$$

The equivalent control quantity is derived from the previous equation:

$$V_{sd}^{eq} = \left(\dot{I_{sd}^{ref}} + \frac{1}{\delta L_s}\left(R_s + \frac{R_r M^2}{L_r^2}\right) I_{sd} - \omega_s I_{sq} - \frac{1}{\delta L_s}\frac{R_r M}{L_r^2}\phi_{rd} \right. \quad \text{(III.34)}$$

$$\left. - \frac{1}{\delta L_s}\frac{M}{L_r}\omega_r\phi_{rq}\right)\cdot \delta L_s$$

We substitute equation (III. 33) into (III. 31), the equation becomes:

$$\dot{S}(I_{sd}) = -\frac{1}{\delta L_s} V_{sd}^{d} \quad \text{(III.35)}$$

During the convergence mode, for the condition $\dot{V}(x) = S(x).\dot{S(x)} < 0$ to be verified, we pose:

$$V_{sd}^{d} = K_{V_{sq}} \cdot signe(S(I_{sd})) \quad \text{(III.36)}$$

Replacing V_{sq}^{d} with its value:

$$\dot{S}(I_{sd}) = -\frac{1}{\delta L_s} V_{sd}^{d} = -\frac{1}{\delta L_s} K_{V_{sq}} \cdot signe(S(I_{sd})) \quad \text{(III.37)}$$

III.8.2 Adjustment of current I_{sq}

The surface expression is:

$$S(I_{sq}) = I_{sq}^{ref} - I_{sq} \quad \text{(III.38)}$$

The derivative of the expression:

$$\dot{S}(I_{sq}) = \dot{I_{sq}^{ref}} - \dot{I_{sq}} \tag{III.39}$$

From (II-39), we have :

$$\frac{dI_{sq}}{dt} = -\frac{1}{\delta L_s}\left(R_s + \frac{R_r M^2}{L_r^2}\right) I_{sq} - \omega_s I_{sd} + \frac{1}{\delta L_s}\frac{R_r M}{L_r^2}\phi_{rq} - \frac{1}{\delta L_s}\frac{M}{L_r}\omega_r \phi_{rd} + \frac{1}{\delta L_s} V_{sq} \tag{III.40}$$

By substituting Equation (I.38) into Equation (III.37), the derivative of the surface becomes:

$$\dot{S}(I_{sd}) = \dot{I_{sd}^{ref}} - \left(-\frac{1}{\delta L_s}\cdot\left(R_s + \frac{R_r M^2}{L_r^2}\right) I_{sd} + \omega_s I_{sq} + \frac{1}{\delta L_s}\frac{R_r M}{L_r^2}\phi_{rd} + \frac{1}{\delta L_s}\frac{M}{L_r}\omega_r \cdot \phi_{rq} + \frac{1}{\delta L_s} V_{sd}\right) \tag{III.41}$$

By replacing the voltage V_{sd} with $V_{sd} = V_{sq}^{eq} + V_{sq}^{d}$, the (III.41) will be written in the following form:

$$\dot{S}(I_{sd}) = \dot{I_{sd}^{ref}} - \left(-\frac{1}{\delta L_s}\left(R_s + \frac{R_r M^2}{L_r^2}\right) I_{sd} + \omega_s I_{sq} + \frac{1}{\delta L_s}\frac{R_r M}{L_r^2}\phi_{rd} + \frac{1}{\delta L_s}\frac{M}{L_r}\omega_r \phi_{rq} + \frac{1}{\delta L_s} V_{sq}^{eq} + \frac{1}{\delta L_s} V_{sq}^{d}\right) \tag{III.42}$$

During the sliding mode and in steady state, we have:

$$S(I_{sd}), \dot{S}(I_{sd}),\ V_{sd}^{d} = 0 \tag{III.43}$$

The equivalent control quantity is derived from the previous equation:

$$V_{sd}^{eq} = \left(\dot{I_{sd}^{ref}} + \frac{1}{\delta L_s}\left(R_s + \frac{R_r M^2}{L_r^2}\right) I_{sd} - \omega_s I_{sq} - \frac{1}{\delta L_s}\frac{R_r M}{L_r^2}\phi_{rd} - \frac{1}{\delta L_s}\frac{M}{L_r}\omega_r \phi_{rq}\right) \cdot \delta L_s \tag{III.44}$$

During the convergence mode, for the condition $\dot{V}(x) = S(x).\dot{S(x)} < 0$ to be verified, we posit:

$$V_{sq}^{d} = K_{V_{sq}} \cdot signe(S(I_{sq})) \tag{III.45}$$

Replacing V_{sq}^{d} with its value in $\dot{S}(I_{sd})$, we find:

$$\dot{S}(I_{sq}) = \frac{1}{\delta L_s} V_{sq}^{d} = \frac{1}{\delta L_s} K_{V_{sq}} \cdot signe(S(I_{sq})) \tag{III.46}$$

III.9. Simulation results

In this section, a numerical simulation was used to illustrate the performances of PV-ELMS control algorithm shown in Figure III.2. The parameters of the asynchronous motor are summarized in Appendix. A stand-alone PV system was simulated using the proposed ELMS to perform dynamic analysis under constant irradiation and temperature levels (1000 W/m^2 and 25^{0}C). During this test, the speed is set to 120 rad/s, then is increased to 150 rad/s at t=1s.

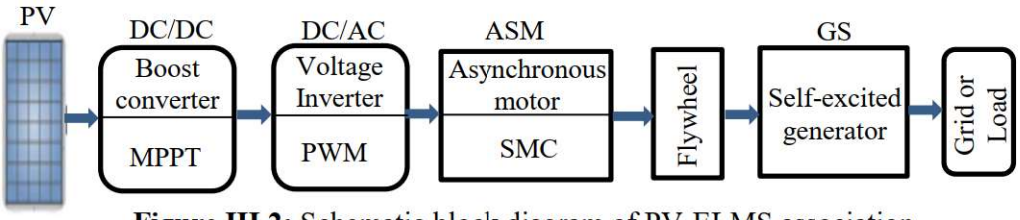

Figure.III.2: Schematic block diagram of PV-ELMS association

III.9.1. Temperature Influence

Figures III.3 and III.4 illustrate the current-voltage and power-voltage characteristics for various temperatures and constant irradiation.

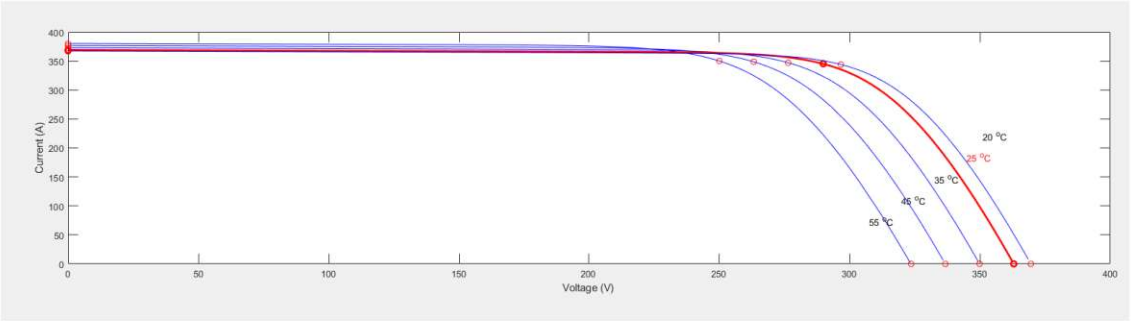

Figure III.3: Current-voltage characteristics at different temperatures and constant irradiation (G=1000W/m²)

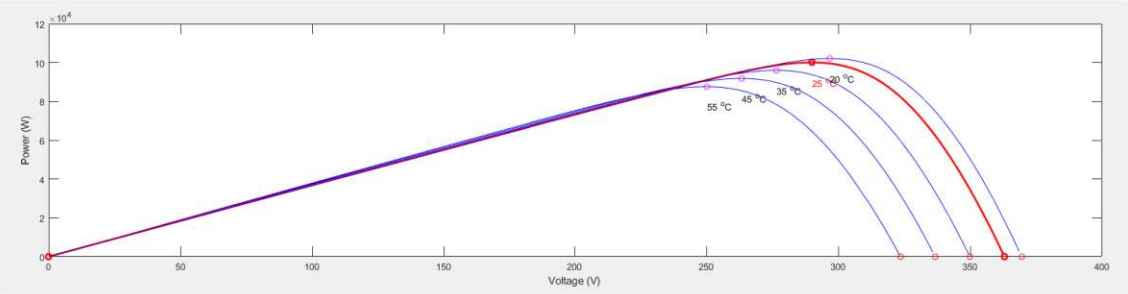

Figure III.4: Power-voltage characteristics at different temperatures and constant irradiation (G=1000W/m²)

Figures III.3 and III.4, show the PV module's current-voltage and power-voltage characteristics. As the temperature rises, so does the current, although the voltage and power fall slightly.

III.9.2. Irradiation effect

Figures III.5 and III.6 illustrate the current-voltage and power-voltage characteristics for various irradiation and constant temperature.

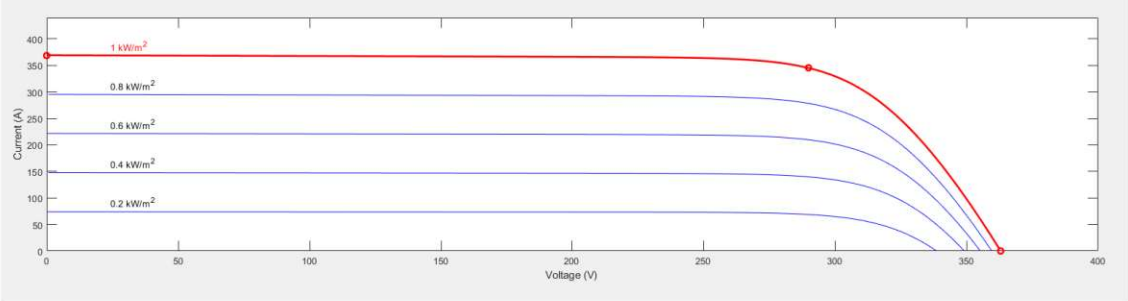

Figure III.5: Current -voltage characteristics at different irradiations and constant temperature (T=25°C)

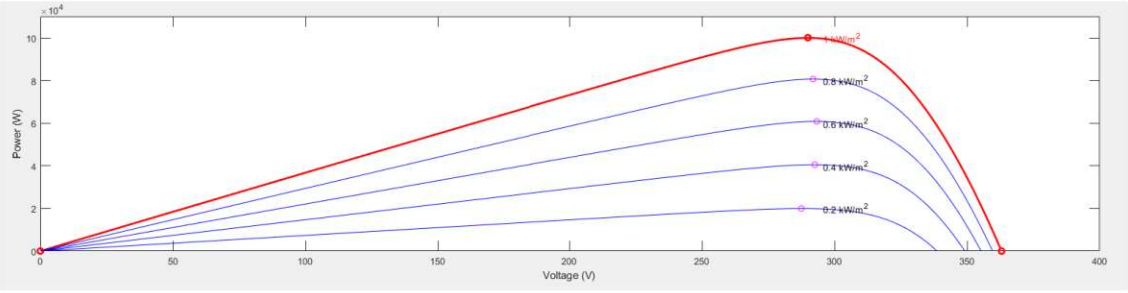

Figure III.6: Power-voltage characteristics at different irradiations and constant temperature (T=25°C)

Figures III.5 and III.6 exhibit results findings for the PV module's current-voltage and power-voltage characteristics, respectively. Increased irradiance causes a significant increase in both current and power, but voltage remains relatively constant.

The I(V) and P(V) characteristics illustrated by Figures III.3-III.6 represent the influence of the increase in temperature on the decrease in the voltage of the solar panel and obviously on its energetic output.

III.9.3. Simulation results for PV-ELMS

Figure III.7 illustrates a simulation of PV system integrated with DC/DC boost converter employing the Perturb and Observe (P&O) MPPT controller.

This result shows DC-link voltage to provide power input to ASM.

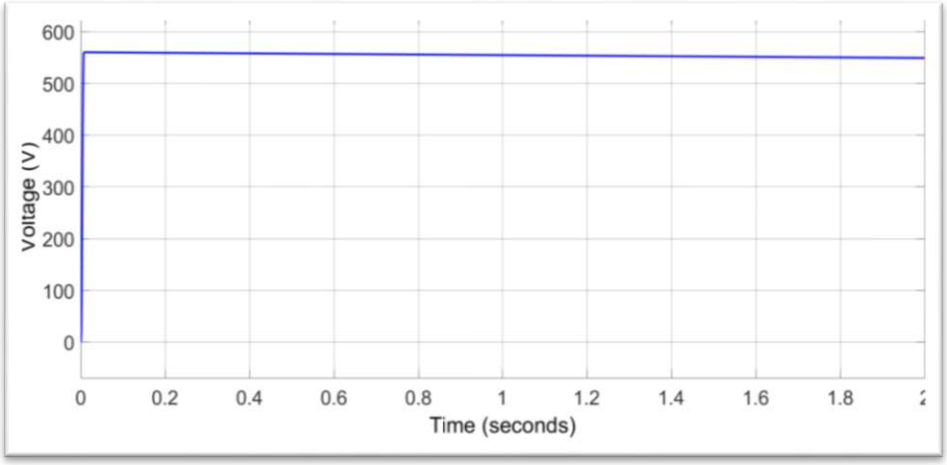

Figure III.7: Output DC voltage of boost converter.

This output voltage of DC/DC boost converter, which increases the voltage of the PV system.

To produce an output voltage close to the sinusoid, we used the inverter PWM control. After the simulation, we obtained at the output of the inverter the signals composed of the three phases as shown in Figure III.8.

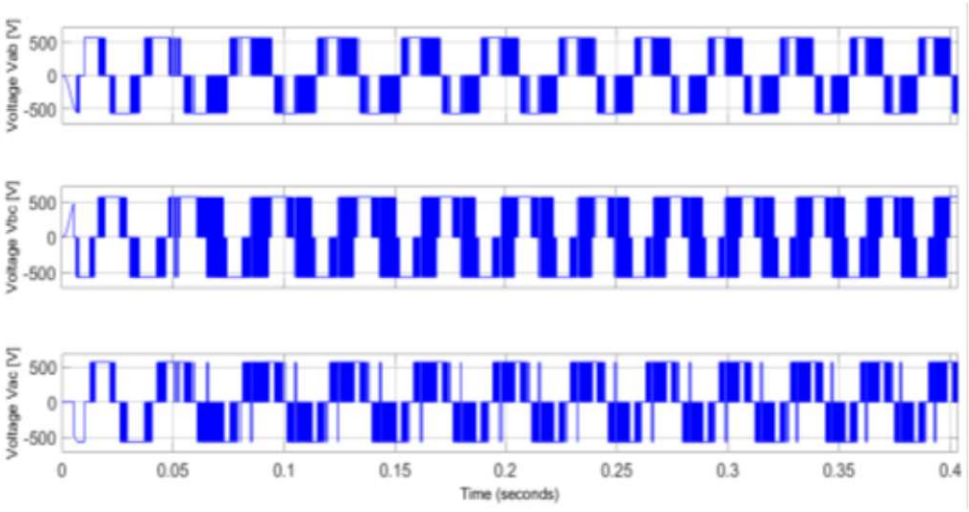

Figure III.8: Inverter output voltages

.

Then, the Figures III.9 and III.10 illustrate the rotor speed and rotor flux of ASM respectively.

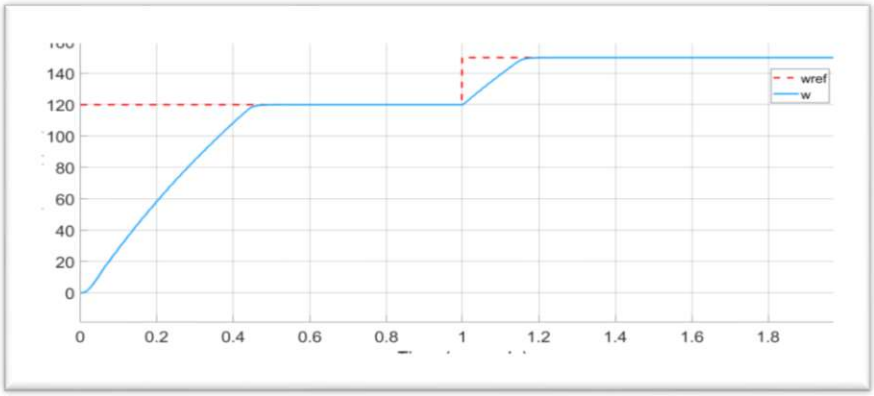

Figure.III.9: ASM Rotor speed.

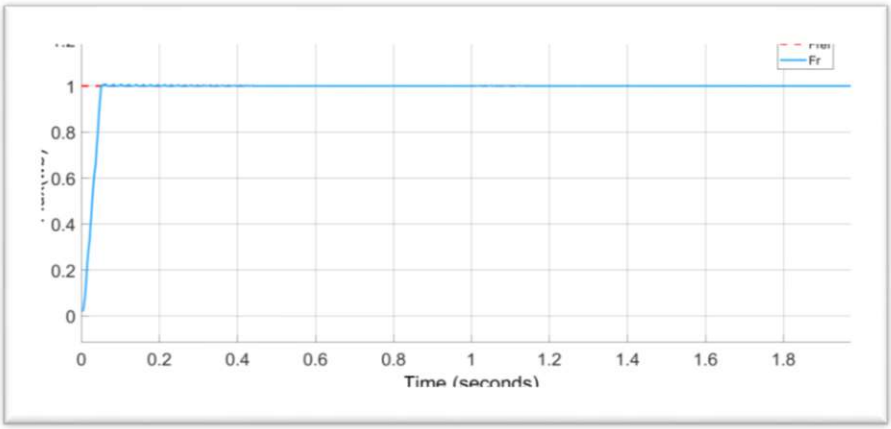

Figure III.10: ASM Rotor flux.

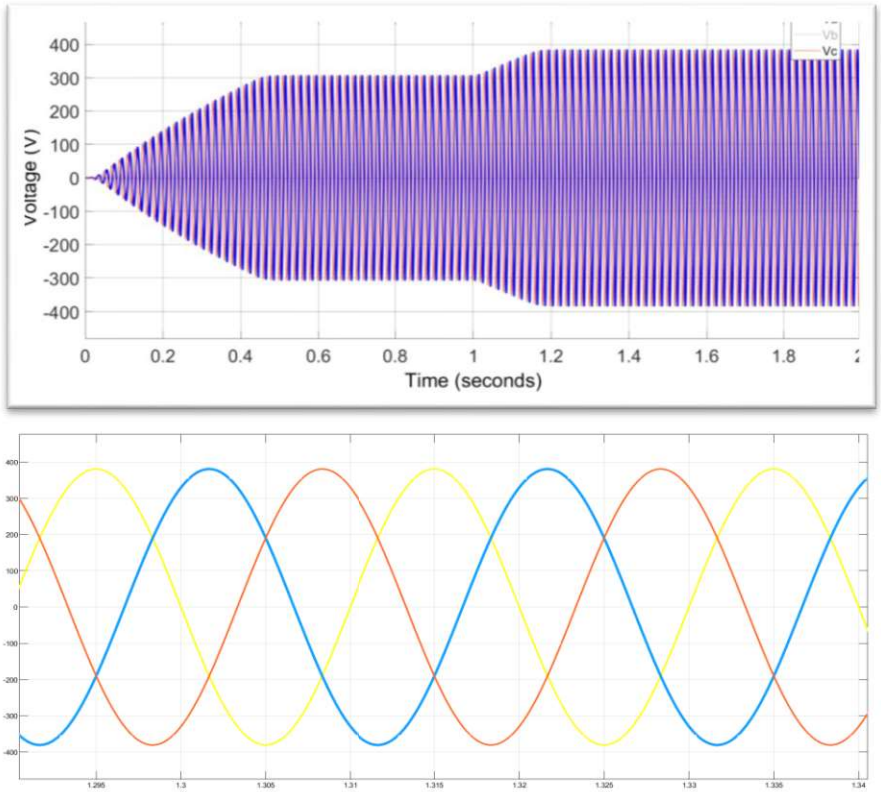

Figure III.11: SG output - three phase voltage and its zoom.

Figure III.11 and its zoom shows result of the output SG self-exited, which is the responsible of the electricity generation as we used.

According results simulation, we have recorded a good response for rotor speed, rotor flux, and three phase voltages output of SG, when we have a variation speed. These obtained results confirm that the control scheme, even at low and high speeds, has good robustness and tracking performance.

III.10. Conclusion

In this chapter, we presented control the asynchronous motor by sliding mode control, also the simulation of the global system. The stand-alone PV system using the P&O MPPT controller. The simulation results show that the PV-ELMS association present a good dynamics performance and his robustness with speed and load torque variation.

General Conclusion

General conclusion

The work carried out as part of this thesis made it possible to study and to control an autonomous photovoltaic system. To do this, we paid particular attention to the development of the different models of the components constituting the system.

At first, our study concerned the photovoltaic effect as well as the current-voltage and power-voltage characteristics of a mathematical model of a single-diode cell. This approach allows us to simulate the behavior of a solar panel and to gain insight into the operation of a photovoltaic field and a photovoltaic generator. We also examined the modeling of the asynchronous machine, flywheel, as well as the model of the synchronous generator and their simulations. The test simulation results confirmed the performance of the proposed method.

To continuously extract the maximum available power from the PV and deliver it to the asynchronous motor through a voltage inverter, a boost converter has been associated and must be controlled by a maximum power point tracking algorithm. In this case, we focused solely on the application of the Perturb and Observe algorithm as it is simple and efficient. Then, to control the ASM we used the sliding mode control technique because it resulted in a good performance.

We concluded that the presence of power electronics is essential in the photovoltaic system to adapt and ensure its proper operation. The inverter typically generates harmonics that can disturb the system. Therefore, filtering them is necessary in this case. As for the presence of the flywheel, it serves to store kinetic energy and ensure the continuity of the system.

Finally, as perspectives, a follow-up work could be enriched by:

- Studying the sizing of the storage to ensure the autonomy of the system.
- Experimenting realization of this bench.
- Developing another control technique to achieve hybrid storage for this system.
- Connecting this system in real time with the grid.

Appendix

APPENDIX

Table 1. Parameters of the asynchronous motor

Nominal parameter	Value
Nominal power	1 Kw
Rotor resistance	6.3Ω
Stator resistance	10Ω
Rotor inductance	0.4612H
Stator inductance	0.4642H
Magnetizing inductance	0.4212H
Inertia moment	0.02$kg.m^2$

Table 2. Parameters of the synchronous generator

Nominal parameter	Value
Nominal power	1 Kw
Rotor resistance	10 Ω
Stator resistance	0.48 Ω
Rotor inductance	0.0231 H
Stator inductance	0.0231 H
Mutual inductance	0.0924 H
Inertia moment	0.263 $kg.m^2$

References

References

[1] BOUNACEUR AMIN, Etude et conception d'un système hybride de production d'énergie, mémoire de master. Université KM Ouargla. 2015.

[2] KECIRI Massinissa, BENMESSAOUD Nassim, Etudes et maximisation de puissance d'un système photovoltaïque, mémoire de master. Université de Bejaïa.2014

[3] Ionel Vechiu, MODELISATION ET ANALYSE DE L'INTEGRATION DES ENERGIES RENOUVELABLES DANS UN RESEAU AUTONOME, Thèse de doctorat. Université du Havre, 2005.

[4] FELLAH Boumediene, Système hybride photovoltaïque-éolien de production d'électricité. Application aux sites de Tlemcen et de Bouzaréah, Thèse de magister. Université de Tlemcen. 2012

[5] Demirbas A. Recent advances in biomass conversion technologies. Energy Educational Science and Technology 6:19–40, 2000.

[6] Rathore NS, Panwar NL. Renewable energy sources for sustainable development. New Delhi, India: New India Publishing Agency; 2007.

[7] Moses, M. (2020, July 02). edf. Retrieved from edfenergy: https://www.edfenergy.com/energywise/renewable-energy-sources N.L. Panwar, S. K. (2011). Role of renewable energy sources in environmental protection: A review. Elsevier, 1513-1514.

[8] MAYOUF Somia, Modélisation et simulation d'un système photovoltaïque connecté au réseau électrique avec une commande vectorielle, mémoire de master. Université Mohamed Boudiaf - M'SILA. 2016.

[9] MECHALIKH Med Nadjib, HAMADA Charaf Eddine, Modélisation et simulation d'un système photovoltaïque en fonctionnement autonome et connecté au réseau, mémoire de master. Université de Ourgla. 2013.

[10] Pascal Pernet, Développement des cellules solaires en silicium amorphe de type « N.I.P » sur substrats souples. Ecole polytechnique fédérale de Lausanne, Thèse de doctorat, 2000.

[11] Chelabi Anis et Ibelhoulen Aziz, Etude d'un système hybride autonome, mémoire de master. Université de Bejaia. 2012.

[12] AL IDRISSI Ramzi, Dimensionnement d'une installation photovoltaïque raccordée au réseau, Rapport de stage de fin d'études, EST Fès. Année universitaire 2015-2016.

[13] Arnaud Sivert, PANNEAUX PHOTOVOLTAÏQUES Etude d'une valise solaire, IUT Génie Electrique & Informatique Industriel de Soissons. Iutenligne, le catalogue de ressources de l'enseignement technologique universitaire.12 mars 2019.

[14] Olivier GERGAUD, Modélisation énergétique et optimisation économique d'un système de production éolien et photovoltaïque couplé au réseau et associé à un accumulateur, Thèse de doctorat en électrotechnique. Ecole normale supérieure de Cachan. 2002.

[15] NAKOUL Zakia, OPTIMISATION D'UNE CENTRALE SOLAIRE A BASE D'UN GENERATEUR PV [Application Aux Sites Tlemcen Et Bouzaréah], mémoire de magister. Université de Tlemcen. 2010

[16] F. TAZERART, R. ABDELLI, GESTION D'UN SYSTÈME PHOTOVOLTAÏQUE AVEC STOCKAGE, mémoire de master. Université de Bejaïa. 2016.

[17] Karimi, M., Mokhlis, H., Naidu, K., Uddin, S. and Bakar, A.H.A. Photovoltaic penetration issues and impacts in distribution network–A review. Renewable and Sustainable Energy Reviews, 53, 594-605, 2016.

[18] I. E. Commission. Characteristics of the utility interface for photovoltaic (PV) systems. Report of IEC, vol. 61727, 2002.

[19] I. S. C. Committee. IEEE Standard for Interconnecting Distributed Resources with Electric Power Systems. IEEE Std, pp. 1547–2003, 2009.

[20] B. N. Alajmi,. Design and control of photovoltaic systems in distributed generation. PhD Thesis, University of Strathclyde, 2013.

[21] Chelabi Anis et Ibelhoulen Aziz, Etude d'un système hybride autonome, mémoire de master. Université de Bejaia. 2012.

[22] J R Cardoso, M B C Salles and M C Costa, Electromechanical Energy Conversion Through Active Learning, 2020, São Paulo, IOP Publishing

[23] F.Gieras, J. (2016). Title: Electrical machines : fundamentals of electromechanical energy.

[24] Foster, L. (2023, 02 21). m-tek assembly ltd. Retrieved fromhttps://www.mtek.co.uk/

[25] Bouchareb Khaled & Chelghoum Abdelmouiz, Etude, modélisation et simulation d'une Machine asynchrone, mémoire de master. Université de Ouargla, 2020.

[26] James, L. (2024, 03 13). Retrieved from power and beyond: https://www.power-and-beyond.com/

[27] Vikram Singh, Shahnawaz Akbar, Hoshiyar Singh. Energy Free Flywheel. International Journal of Research Publication and Reviews, 2023.

[28] BELFEDHAL Abdelmalek, Etude et Simulation d'une Centrale Photovoltaïque Connectée au Réseau Electrique a la Région d'Adrar, mémoire de Magister. Université d'Adrar. 2013.

[29] Marcelo Gradella Villalva, Jonas Rafael Gazoli, and Ernesto Ruppert Filho, Comprehensive Approach to Modeling and Simulation of Photovoltaic Arrays. IEEE TRANSACTIONS ON POWER ELECTRONICS, VOL. 24, NO. 5, MAY 2009.

[30] M. G. Villalva, J. R. Gazoli, E. Ruppert F, Modeling and Circuit-Based Simulation of Photovoltaic Arrays. Brazilian Journal of Electronics, vol. 14, no. 1, pp. 35-45, ISSN 1414-8862, 2009.

[31] ZIGHA ALI, ETUDE ET SIMULATION D'UN SYSTEME HYBRIDE PHOTOVOLTAÏQUE-EOLIEN, mémoire de master. Université Constantine. 2013.

[32] Djamila CHERIFI, Estimation de la vitesse et de la résistance rotorique pour la commande par orientation du flux rotorique d'un moteur asynchrone sans capteur mécanique. Université des Sciences et de la Technologie d'Oran Mohamed Boudiaf. Juin 2014.

[33] NAAR Mustapha, ARBAOUI Fayçal, Commande par mode flou-glissement de la machine asynchrone, mémoire d'ingénieur d'état. Centre universitaire de Bechar .2005

[34] Adjimi Nadia, Belaidi Wahiba, Modélisation et commande d'un onduleur MLI. Universitaire Oum El-Bouaghi. 2009.

[35] Rachid ABDESSAMED, Modélisation et simulation des machines électriques, livre, Ellipses Edition. ISBN 978-2-7298-6495-8. Paris. 2011.

[36] G.-O. Cimuca, « Système inertiel de stockage d'énergie associé à des générateurs éoliens », THESE, Arts et Métiers ParisTech, 2005.

[37] G. Genta, Kinetic Energy Storage: Theory and Practice of Advanced Flywheel Systems. Butterworth-Heinemann, 2014.

[38] J. KAUV et J. BONAL, « Stockage inertiel de l'énergie », Tech. Ing., févr. 2012.

[39] « rosseta Technik GmbH », 22-janv-2013. [En ligne]. Disponible sur: http://www.rosseta.de/. [Consulté le: 22-janv-2013].

[40] OTMANE CHERIF Anis, Observation de la Machine Synchrone à Rotor Bobiné Sans Capteurs (Sensorless), mémoire de Master. Université Mouloud MAMMERI, Tizi-Ouzou. 2016.

[41] Radhwane SADOUNI, Abderrahmane BELLAOUAR, Commande par Mode Glissant de la Machine Asynchrone Double Etoile, Laboratoire des Matériaux, Technologie des Systèmes Energétiques et Environnement, Université de Ghardaia, 2020.

[42] A.Meroufel, «Commande découplée d'une machine asynchrone sans capteur mécanique », Thèse de doctorat d'état, Université de Sidi Bel Abbes, 2004.

[43] Taleb Moustapha Ould Abdou «Commande par mode de glissement floue avec observateur application à différents pendules inversés », mémoire de magister, (E.N.P) ,2006.

[44] Reffa Sabiha,Bensafi Adel, « Commande par mode glissant de la machine asynchrone », mémoire de master, centre universitaire Belhadj Bouchaib, 2016.

Abstract:

The subject is part of significant improvements in the production of electrical energy, more particularly to increase energy yields based on an electromechanical system (ELMS) while contributing to the establishment of essential commercial institutions and frameworks, in the gas and energy sector. To achieve this objective, the solution is to couple the ELMS and the energy storage system.

In this thesis, we interested in the flywheel, a storage system allowing the conversion of electrical energy into kinetic form and vice versa based on a self-excited synchronous generator. The flywheel is driven by an asynchronous motor coupling a photovoltaic field. In this study, the test system is presented as well as the results obtained in closed loop on the system performance.

Keywords: Photovoltaic Generator (PV), Sliding Mode Control (SMC), Asynchronous Motor (ASM), Flywheel, Synchronous Generator (SG).

Résumé :

Le sujet s'inscrit dans le cadre d'améliorations importantes au niveau de la production de l'énergie électrique, plus particulièrement pour augmenter les rendements énergétiques à base d'un système électromécanique (SELM) tout en contribuant à la mise en place d'institutions et cadres commerciaux essentiels dans le secteur gazier et énergétique. Pour atteindre cet objectif, la solution est de coupler le SELM et le système de stockage d'énergie.

Dans ce mémoire, nous nous sommes intéressés au volant d'inertie, système de stockage permettant de convertir l'énergie électrique sous forme cinétique et vice versa à base d'une génératrice synchrone auto-excité. Le volant d'inertie est piloté par un moteur asynchrone couplant un champ photovoltaique. Dans cette étude, le système de test est présenté ainsi que les résultats obtenus en boucle fermée sur les performences système.

Mots Clés: Générateur photovoltaïque, Commande mode glissant, Moteur asynchrone, Volant d'inertie, Génératrice synchrone.

ملخص:

الموضوع يندرج في إطار التحسينات الهامة في إنتاج الطاقة الكهربائية، وتحديداً لزيادة كفاءات الطاقة عن طريق نظام كهروميكانيكي مع المساهمة في إنشاء المؤسسات والأطر التجارية الأساسية في قطاع الغاز والطاقة. لتحقيق هذا الهدف، الحل هو ربط نظام كهروميكانيكي ونظام تخزين الطاقة. في هذا السياق، قمنا بدراسة عجلة العزم، نظام تخزين الطاقة الذي يحول الطاقة الكهربائية إلى طاقة حركية والعكس بناءً على مولد متزامن ذاتي التحفيز. تتحكم عجلة العزم بواسطة محرك غير متزامن يربطها بمجال الطاقة الشمسية. في هذه الدراسة، يتم عرض نظام الاختبار والنتائج المحصل عليها في حلقة مغلقة حول أداء النظام.

الكلمات المفتاحية : مولد كهروضوئي , تحكم انزلاقي , محرك غير متزامن , عجلة العزم , مولد متزامن .